

Article

Mould-Growth Study in Building Materials Exposed to Warm and Humid Climate Using Heat and Mass Transfer (HAMT) EnergyPlus Simulation Method

Shoumik Desai ¹, Naga Venkata Sai Kumar Manapragada ², Anoop Kumar Shukla ^{2,*} and Gloria Pignatta ^{3,*}

¹ NITTE Institute of Architecture, Mangalore (NITTE DU), Mangaluru 575018, Karnataka, India; shoumik.desai@gmail.com

² Manipal School of Architecture and Planning, Manipal Academy of Higher Education, Manipal 576104, Karnataka, India; nagavsk.m@manipal.edu

³ School of Built Environment, Faculty of Arts, Design and Architecture, University of New South Wales (UNSW), Sydney, NSW 2052, Australia

* Correspondence: anoopgeomatics@gmail.com (A.K.S.); g.pignatta@unsw.edu.au (G.P.)

Abstract: Commercial energy consumption currently accounts for 8.6% of the total national energy consumption in India and it is predicted to surge in upcoming years. To tackle this issue, building envelope insulation is being promoted through codes and standards to reduce the cooling and heating demand and hence reduce the overall energy demand. However, with prolonged exposure to humid ambient conditions in warm-humid locations, building materials undergo decay in their hygrothermal properties, which induces mould growth and increases the energy that is needed to tackle the latent cooling load. Mould growth, in turn, harms the occupant and building health. Therefore, this study attempts to evaluate the mould-growth index (MGI) in the coastal city of Mangalore, Karnataka, India using the heat and mass transfer (HAMT) model. The MGI for one autoclaved aerated concrete (AAC) wall assembly in a representative commercial building has been studied by integrating EnergyPlus through the Python plugin. The simulated results suggest that the annual mean MGI for the AAC assembly is 3.5 and that mould growth will cover about 30–70% of the surface area. Furthermore, it was concluded that surface temperature, surface humidity, and solar radiation are key parameters for mould growth on the surface of a material.

Keywords: HAMT model; mould-growth index (MGI); commercial buildings; numerical simulations; indoor dampness; water content; hygrothermal properties; insulation; building materials; Mangalore



Citation: Desai, S.; Manapragada, N.V.S.K.; Shukla, A.K.; Pignatta, G. Mould-Growth Study in Building Materials Exposed to Warm and Humid Climate Using Heat and Mass Transfer (HAMT) EnergyPlus Simulation Method. *Sustainability* **2022**, *14*, 8292. <https://doi.org/10.3390/su14148292>

Academic Editor: Antonio Caggiano

Received: 19 April 2022

Accepted: 22 June 2022

Published: 6 July 2022

Publisher's Note: MDPI stays neutral with regard to jurisdictional claims in published maps and institutional affiliations.



Copyright: © 2022 by the authors. Licensee MDPI, Basel, Switzerland. This article is an open access article distributed under the terms and conditions of the Creative Commons Attribution (CC BY) license (<https://creativecommons.org/licenses/by/4.0/>).

1. Introduction

India is the seventh-largest country in the world with a reported 132% rise (80 TWh to 186 TWh) in domestic energy consumption between the years 2000 and 2012. Commercial energy consumption accounts for 8.6% of the total national energy consumption and it is predicted to rise at an annual rate of 5% in the coming years [1]. Energy consumption in the commercial sector is also predicted to increase due to the $\approx 400\%$ (about $2 \times 10^{10} \text{ m}^2$) upsurge in the cumulative floor area of new buildings by 2030 [2]. In addition, as India's gross domestic product (GDP) continues to rise, consumer purchasing power is expected to increase too, leading to higher demands for comfort in buildings [3].

The need for energy has been rising globally. The higher thermal comfort expectations that are placed on buildings are directly related to an increase in the cost of energy, as well as energy demand. This encourages a wider choice of insulating products to be used. The amount of energy that is required to heat or cool the indoor environment can be reduced by installing insulation, resulting in fewer greenhouse gas emissions and reduced monthly energy expenses for heating and cooling. Insulation is also considered to be the first element of defence for mould prevention and its effectiveness is determined by thickness, type,

and where it is placed, as well as the conditions in which it is stored. High temperatures and relative humidity combined with the presence of biodegradable material contribute to creating the best conditions for mould growth. This means that the prolonged exposure of organic insulation materials (or dust and organic materials that are present on the surface of the building envelope) to humidity and precipitation can lead to mould growth, along with a considerable loss of insulating qualities [4–6].

Within and between countries, continents, and climate zones, the prevalence of indoor dampness varies greatly. In India, indoor dampness is expected to affect 10–50% of built-up space [7]. Situations of dampness are extremely severe in specific environments such as river valleys and coastal areas and are usually much worse than the national norms for such conditions. The amount of water that is present on or in materials is the most critical factor in stimulating microorganism growth, including fungi, actinomycetes, and other bacteria. Most of the peninsular coasts of Indian cities are categorized under the warm-humid climate, where the mean summer and winter temperature varies between 25 °C and 35 °C, and 20 °C and 30 °C, respectively, whereas the mean relative humidity (RH%) ranges between 70–90% throughout the year [8]. This implies that the prevailing climate conditions in the coastal cities of India result in the buildings becoming highly susceptible to mould growth [7]. It is also estimated that about 75% of the buildings constructed in India suffer from waterproofing problems [7]. This results in improper remediation measures and unhygienic conditions, again helping to develop indoor dampness in buildings. A questionnaire-based study, conducted in 700 houses—both rural and urban—in the Indian state of Tamil Nadu, aimed to identify the major sources of household dampness. The study reported that dampness based on residents' perceptions was identified in 353 houses, about 50% of the studied houses [9].

Dampness or excess moisture is defined as a moisture state variable that is higher than a design criterion. It is usually represented as moisture content [10]. The building-material selection criteria can either be simple or complex parameters such as surface condensation and visible scales on the building due to prolonged exposure to humidity. On the other hand, complex parameters include the continuous fluctuation of moisture, i.e., a mould-growth index [11,12]. The mould-growth index (MGI) can be used to evaluate the probability of magnitude of mould growing on a surface [11,13,14]. MGI is a mathematical-empirical model that forecasts mould growth on building materials as a function of substrate material, temperature, and relative humidity. MGI is a seven-point scale from 0 to 6, with 0 indicating no mould growth and 6 indicating very heavy and dense growth. Its physical characteristics have been reported in [11] and summarized in Table 1.

Table 1. Table showing the mould-growth index and its corresponding physical characteristics [11].

Mould Index	Covered Area [%]	Typical Feature
0	0	No mould growth
1	≤1	Mould growth is very little, only observable under a microscope
2	≤5	Moderate mould growth that can only be observed under a microscope
3	<10	Visually observable mould growth
4	>10 and <50	Visually observable and dense mould growth
5	>50	Prolific growth on the surface
6	100	Heavy and dense growth

Additionally, mould growth is a function of three primary variables: water activity (A_w), equilibrium relative humidity (ERH), and moisture content (MC), which are discussed further. Water activity (A_w) refers to the level of dampness that is required for mould to grow. This is a measurement of how much moisture is accessible for microbiological growth and it is calculated by dividing the vapour pressure of the substrate by the vapour pressure of pure water at the same temperature. This can alternatively be stated as a ratio of the water-vapour pressure of the amount of water in a substance to the water-vapour pressure of pure water [15–19]. For example, the A_w will be 0.6 if the vapour pressure of the water in a substance is 60% that of pure water (or the saturated material). Furthermore, the

equilibrium relative humidity (ERH) relation can be understood by placing the building construction material in a closed system, allowing the air in the system to attain moisture balance with the material, then determining the RH and multiplying by 100, as explained in Figure 1 and Equation (1) [19,20].

$$A_w = \frac{P}{P_0} \quad (1)$$

where A_w is water activity; P is vapour pressure on the material at a given temperature; and P_0 is pure water-vapour pressure at the same temperature.

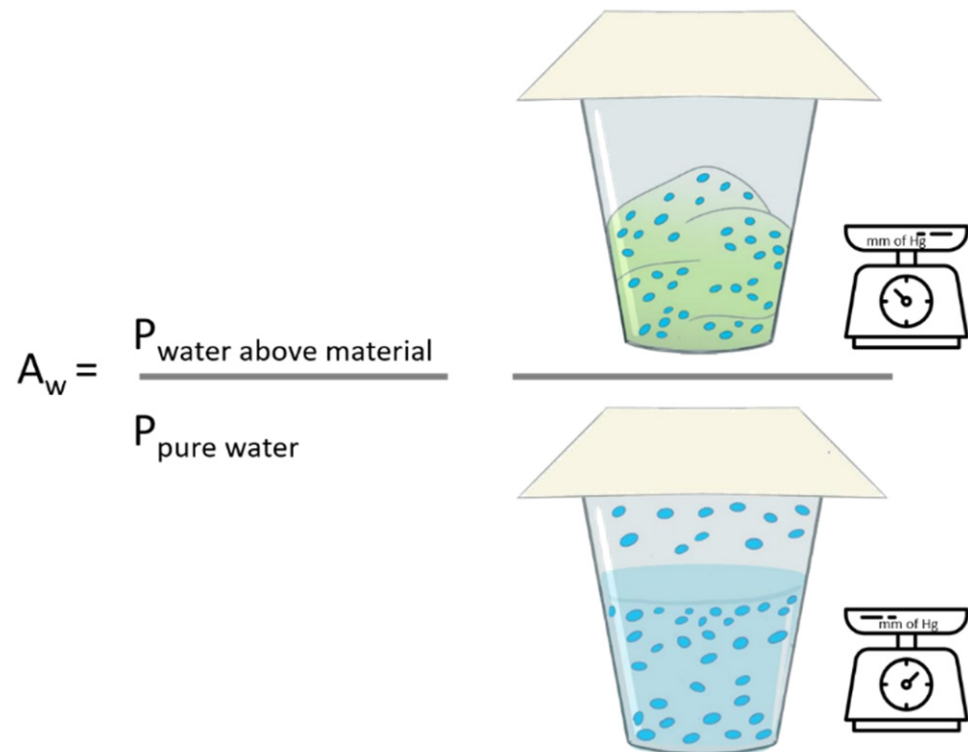


Figure 1. Showing the concept of water activity. (Source: authors.)

When the RH of the air is in equilibrium with the RH at the surface of a material it is known as the equilibrium relative humidity (ERH). This ERH is expressed as a percentage and ranges from 0% to 100%. The ERH can be measured when the surface RH and the ambient RH are in equilibrium. This can be achieved by placing a small plastic tent on any surface and then inserting an RH sensor into the tent. This arrangement allows the confined air to attain equilibrium with the surface. Note that the edges of the plastic tent should be sealed so that equilibrium is achieved. This generally takes about 10–15 min.

As the relative humidity of the air at the surface of a material and that of the surrounding air stabilizes, it can be said that an equilibrium relative humidity has been achieved at that temperature. This has been explained in Figure 2 and Equation (2) [19,20].

$$\text{ERH (\%)} = A_w \times 100 \quad (2)$$

where ERH is the equilibrium relative humidity and A_w is water activity.

Moisture content (MC) is defined as the mass of moisture in a substance with its dry mass, expressed as a percentage. For example, if a brick weighs 500 g when dry and contains 50 g of water, the brick has an MC of 10% [16,19,20]. The moisture content can be measured using pinless or pin-type moisture meters. The earliest type of method is weight loss on drying which is an analytical method. However, pin-type moisture meters are commonly used for field determination of the material moisture content. The pin meter measures the

moisture indirectly by measuring the resistance (conductance) with an electrical current that goes from one pin to the other. The moisture content is measured by gently inserting the pin meter into a surface perpendicularly, and with each repeated measurement a new hole should be considered. The moisture content meter gives immediate results on a display screen and is independent of the ambient temperature. A simple working representation of the moisture content meter is shown in Figure 3.

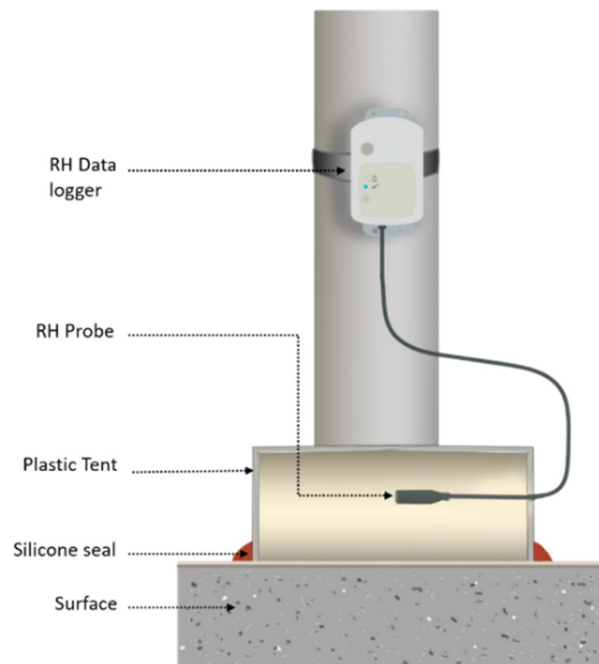


Figure 2. Equilibrium relative humidity (ERH) can be measured at the surface by sealing a tent to the surface and measuring the RH inside the tent. (Source: authors).



Figure 3. Measurement of a surface's moisture content. (Source: authors).

The dust and dirt that are prevalent in indoor and outdoor environments provide enough nutrients for microbial growth to thrive. Mould fungi are aerobic and specifically need a dry-bulb temperature (DBT) of between 22 and 35 °C, and an RH of between 71 and 95% [17,18]. These combinations of RH and DBT changes in and on building construction works cause water to condense on the exterior and interior surfaces, resulting in the growth of microbes such as mould, fungi, and bacteria, and induce the degradation of the building materials. The pH value, moisture content on the material surface, equilibrium RH, surface temperature, ambient RH, ambient dry-bulb temperature, water activity, indoor and outdoor air velocity, precipitation, the light, roughness of the surface that mould develops on, biotic connections between various cultures, and contact time are all factors that contribute to mould growth [21–24].

A numerical mould-growth model was used to evaluate the response of humidity, temperature, and exposure duration for mould growth on wood material [11,25,26]. This was based on extensive research with Northern wood species in the lab [26]. Adan [21] and Clarke et al. [27] also presented a different mathematical model for mould growth. In recent years, research on modelling moisture and microbiological problems in buildings has been more active [23,28]. Furthermore, Viitanen's mould development model has been found appropriate for examining building structures that are composed of diverse construction materials when tested under varied environmental circumstances [29]. The American Society of Heating, Refrigeration, and Air Conditioning Engineers (ASHRAE) recognized the need to prevent mould growth and developed ASHRAE 160-2009, which addresses Guidelines for Moisture-Control Design Analysis in Buildings. The Position Document on Limiting Indoor Mould and Dampness in Buildings, published in 2012, backed this development, and ASHRAE 160 was further updated in 2016.

The three generally used models for predicting the hygrothermal performance of buildings are WUFI, heat and mass transfer (HAMT), and effective moisture penetration depth (EMPD) [30]. The level of sophistication and runtime requirements differ depending on the tool used. WUFI and HAMT have been reported to have the best hygrothermal capacities, followed by EMPD [27]. It was reported that WUFI could not account for air leakage and transfer at surface boundaries, whereas HAMT is incapable of accounting for air leakage, precipitation-related moisture difficulties, or condensation problems that are caused by high relative humidity. However, it was also found that HAMT, which accounts for transient heat and mass transport, has the most mould-growth modelling potential. Furthermore, HAMT is open-source software, and special features that enable EnergyPlus to model all the essential heat and moisture transfer mechanisms that affect the performance of building envelope components have been prioritized [30].

Mould growth differs depending on the type of building material. Some substrates such as ceramic materials and gypsum board, even when exposed to a temperature of 20°C and an RH of 80–90%, do not support mould growth, while other substrates such as wood, wood composites, and starch-containing materials allow mould growth even at an RH lower than 75%. Several investigations have been carried out to determine the temperatures and humidity levels at which various types of building materials begin to mould [31,32]. The availability of nutrients and the amount of A_w on the surface of the building construction material are both important factors in mould formation. When the right amount of salt or sugar is present on the material's surface or substrate, the mould will grow. These nutritional media are readily available when groundwater rises inside the building due to capillary action, curing during construction, or dust and showers during monsoon seasons [19,21]. Damp buildings and water-damaged building materials and their substrates yield hydrophilic fungi and have a minimum A_w of 0.9, while dry substrates such as common household floor dust and dry wood yield xerophiles and have a minimum A_w of 0.75. At a water activity of 0.75–0.79, moderately xerophilic fungi begin to develop, while mildly xerophilic fungi begin to proliferate at an A_w of 0.80–0.89 [17]. Furthermore, if the A_w of the material is greater than 0.75 for an extended length of time, the risk of mould growth is greater [33].

A_w for different mould development varies depending on the type of mould [34]. Few filamentous fungi, for example, can thrive on a substance with an A_w of 0.78, whereas others may live for 3 weeks with an A_w of 0.45 [35]. It has also been reported that even if nutrient supply is not ideal, mould can still develop if the RH is greater than 90% [36].

Much field work and many laboratory investigations have been conducted to determine the settings and factors under which mould growth occurs on building construction materials. The damaged buildings have been linked to a variety of organisms and bacteria. These organisms can be found in abundance in our surroundings, including dirt, rotting materials, and debris. A number of key points have been collected from this past research and presented below:

- Research that was conducted on the surface of wood found that an ambient RH over 75–80% or an A_w above 0.75–0.80 is crucial for developing mould and fungi on the surface. Moreover, temperature and exposure time both influence the critical humidity level [26];
- Under laboratory settings, the growth of Scots Pine (*Pinus sylvestris* L.) and Norway Spruce (*Picea abies* Karst.) moulds were investigated. The samples were exposed to temperatures of 0 °C, 5 °C, 15 °C, 20 °C, and 30 °C with RH levels of 86–88%, 90–92%, 96–98%, and 99%, and 100%. The mould-growth conditions and decay development of *Coniophora puteana* (*Schum. ex Fr.*), P. Karsten (*BAM Ebw. 15*), a common brown rot fungus, were investigated. A regression model was presented for the crucial response periods of temperature and humidity conditions, and the findings indicated that mould growth was greatly influenced by temperature. The wood was clearly attacked and degraded by *C. puteana*. The samples were further exposed for three months at RH levels of 96–100% and 30 °C, and the study reported that the lowest humidity conditions for decay development must lie above an RH of 90–92% for a 60-month exposure time at 30 °C. Between 0 °C and 5 °C, the lowest humidity conditions for decay development lie around a RH of 97% and the wood moisture content around the fibre saturation point [24];
- In a study investigating various building materials and their durability, Spruce plywood, pine sapwood, fibreboard, gypsum board, concrete and cement screed on concrete, concrete (K30), glass wool, rock wool, and expanded polystyrene (EPS) were among the materials investigated. The tests were conducted in an environmental room with a 98–100% RH, 95–97% RH, and 88–90% RH and a temperature varying between 15 and 23 °C. The results were ranked on seven-point mould indexes. The mould development was monitored every week at first, then every two weeks after that. The samples were then examined under a microscope. When the RH was 95–100% and the DBT was 20 °C, the MGI for organic materials, including pine sapwood, spruce plywood, and particle board was as high as 5–6. Mould growth, on the other hand, was less abundant and slower in clean concrete and thermal insulation samples in similar settings. Mould growth was also slowed in all of the samples when the RH levels were between 88 and 90%. After 12 months of exposure, the materials were shown to have low mould development when exposed to an RH of 78–80% [37];
- In a simulation-based study investigating hygrothermal responses, a 4 m × 4 m × 10 m tower with 0.29 m thick brick walls and a wind-driven rains (WDR) load on the facades were studied. It was reported that mould did not proliferate at an RH greater than 96%, although it can still exist when the effects of WDR are considered. Furthermore, mould growth poses a severe threat, especially in the summer and winter, with the summer being a greater threat than the winter. When the simulation results with WDR loads are compared to those without WDR, it becomes clear that the former conditions greatly impact mould growth at the interior wall surfaces. Additionally, the substrate surface relative-humidity conditions account for a greater risk of mould growth as compared to other parameters such as surface temperature in this study [38];
- Another simulation-based study investigated a 3 m-high cubic construction facing south-east. Instead of a single construction material, the authors simulated two sets

of the wall assembly. Six instances were simulated in total, with two different wall assemblies and three different TMY3 (typical meteorological year) weather settings for the simulation. All three selected locations represented humid conditions, and the outdoor air temperature was above 24 °C for 75% of the time, and above 22 °C for 98% of the time during the summer months of June to August. The target layer was the inner gypsum board. The yearly change in the mould index was determined using the mathematical approach [10]. According to the simulation results, 3 m-high walls facing all directions in an unpressurized building in Easterwood Airport showed a severe annual increase in the mould index for a 22 °C internal temperature set-point. In all of the cases, infiltration was the primary cause of mould growth. Due to the prevailing outdoor warmth and humidity, moist outdoor air enters from the top and exits from the bottom of the wall during the summer months, causing severe mould growth in the upper sections of the wall. Furthermore, the authors recommend that the risk of mould growth should be considered in conjunction with internally generated moisture and exfiltration. Furthermore, the simulated results report that an unpressurized building will have an annual increase in the mould index for a 22 °C indoor setpoint temperature. However, a positive pressure of 1.5 Pa and a 22 °C indoor set-point temperature decreases the risk of mould growth on all the walls [39];

- A mould-growth investigation on ten different building materials (wood-based materials, gypsum boards, and inorganic boards) was performed under controlled laboratory conditions [15]. In addition, a variety of important moisture levels were assessed. This 50 mm × 100 mm sample was injected with spores from six mould fungi species (*Eurotium herbariorum*, *Aspergillus versicolor*, *Penicillium chrysogenum*, *Aureobasidium pullulans*, *Cladosporium sphaerospermum*, *Stachybotrys chartarum*) and incubated in a climate test chamber (CTS C-20/350, CTS GmbH, Hechingen, Germany). The testing settings were at temperatures ranging from 10 to 22 °C, with RH levels ranging from 75 to 95%. Further, every week for 12 weeks, the mould growth on the samples was examined under a stereomicroscope at 10 to 40 times magnification. The study suggested that chipboard, thin hardboard, plasterboards, and asphalt paper were less sensitive to mould growth as compared to plywood and pine sapwood. No growth was identified on glass fibreboard, cement-based board, or extruded polystyrene board samples in any of the settings studied. Table 2 summarizes the mould-growth index results for the investigated materials under various RH and temperature settings;

Table 2. Mould-growth results summarised by week, showing when mould growth was first detected.

Material Name	Temperature [°C]	Week when Mould-Growth Index of ≥ 2 for at Least one Piece Was Found			Week when Mould-Growth Index of Median ≥ 2 Was Found		
		85% RH	90% RH	95% RH	85% RH	90% RH	95% RH
Chipboard	10	-	-	5	-	-	5
	22	7	5	1	7	5	1
Pine sapwood	10	-	8	2	-	9	1
	22	3	2	1	3	3	1
Plywood	10	12	3	2	-	4	2
	22	1	1	1	3	1	1
Thin hardboard	10	-	-	11	-	-	-
	22	-	4	1	-	12	1

- Another study was conducted to evaluate the mould growth on three different materials and different surface treatments in a controlled temporary laboratory environment [40]. Three distinctly different building materials were used in the experiment, each with four different surface treatments. The size of the test samples was 13.5 × 18.5 cm. This resulted in a total of 3 × 4 = 12 distinct combinations. Three replicas and one control sample were used in each combination (a total of 48 samples): (1) aerated cellular concrete (H + H multi-board, thickness 25 mm); (2) gypsum board

(Gyproc GN, thickness 13 mm); (3) oriented strand board (OSB) were chosen as the building materials (Egger OSB3, thickness 15 mm). To represent both organic and inorganic substrates, the following surface treatments were chosen: (1) wood chip wallpaper and paint; (2) wallpaper with a print; (3) paint; (4) non-woven glass felt and paint. The samples were inoculated with eight common indoor fungi that reflect common species seen in water-damaged or wet structures [35]. The RH was measured in steps: 75% RH for 8 h, 98% RH for 2 h, 65% RH for 8 h, and 88% RH for 4 h. The temperature was kept at 20 °C. For 41 weeks, the sample was investigated. These conditions were created to investigate the worst-case scenario that could occur in the housing units during peak cooking and showering hours. For the first week, the samples were monitored daily, then every week. A visual inspection and a stereomicroscope were used to analyse the mould growth. If air mycelium was evident at the inoculation site, the mould development was defined. According to the findings, building materials with a low moisture content of 50% RH are very resistant to mould formation, even when exposed to 90% RH for a short period of time. The material would be sensitive to mould growth if it was exposed to a high RH for an extended time, particularly with organic materials, which contain sufficient nutrients to enable mould growth even at 75% RH. The study concluded that the building materials should be selected so that the indoor surface RH never reaches 75% [40];

- In India, mould samples were collected from three monuments: Agra Fort, the Christian Cemetery, and Kailash Temple in three seasons to evaluate the effect of RH (summer, rain, and winter, with RH 50–60%, 80–98%, and 70–85%, respectively). The data showed that the rainy season had the most fungal variety, followed by winter. Thermophilic fungi occurred in the isolation process throughout the summer season. Using a tropical chamber test, the effect of RH on mould growth was also inferred [41].
- Another study that was conducted in India developed a methodology for preparing a survey form to assess household dampness. For gravimetric testing, the study included on-site readings and disruptive sample-collection procedures [9];
- The impact of moisture-induced variations in thermal conductivity and specific heat capacity on the energy performance of different building envelopes was also investigated. The research was conducted in the lab and analysed using coupled heat and moisture transport computational modelling. According to the findings, the increased moisture content was a significant negative effect impacting both the thermal characteristics of materials and the energy balance of the envelopes. This finding highlights the need to use moisture-dependent thermal characteristics for building materials in energy calculations [42]. Additionally, actively growing mould harms the material it lives on, compromising structural integrity;
- All building materials, in general, have a thermal insulating property. Insulating materials with a thermal resistance (λ) of less than 0.175 W/m·K are effective when used with standard building materials to boost a structure's thermal resistance. Thermal conductivity rises with increasing humidity; as a result, the insulating layer must be kept as dry as possible. However, no building material can be dehydrated in natural conditions. There is always a so-called practical (final) moisture, which slightly degrades a building material's insulating characteristics [4]. The findings show that moisture absorption was a substantial contributor to changes in the materials' thermal characteristics. The degradation of some aerogel blankets and closed-cell polyurethane samples was as high as 15% and 27.5%, respectively [10];
- According to the measurement results, the thermal resistance of expanded polystyrene fell below the Kolmogorov–Smirnov chart (KS) performance limits after around 80–150 days from the date of manufacture. In comparison to the initial thermal resistance, the material's thermal resistance fell by 25.7–42.7% after around 5000 days. In the case of stiff polyurethane, approximately 100 days after manufacture, a pattern of rapid-performance degradation emerged, and the thermal resistance fell below the

- KS performance limits after about 1000 days. After around 5000 days, the thermal resistance had decreased by 22.5–27.4% compared to the initial thermal resistance [43];
- Another study evaluated the biological resistance of a thermo-chemically treated wood of black pine and poplar species under controlled lab conditions. The experiment suggests that thermal treatment increases the organic growth resistance of the black pine by 9–37% as compared to the unmodified wood against *C. puteana*. On the other hand, the thermally treated pine specimens and poplar showed high resistance to organic growth and the lower mass loss was noted at 28–68% and 32–35%, respectively, against *O. placenta* as compared to the unmodified samples. This study further concludes that thermal treatments and chemical treatment such as benzoin and silane solution help to protect the wood and poplar species against mould growth and other forms of degradation of the hygrothermal properties of the material [44].

In addition to the above research, other studies have collected data on the thermo-physical properties [45,46] and embodied energy [47] of building materials. However, determinants like water activity, ERH, and moisture content are not widely studied. Further, there were minimal studies found in the Indian context for the study of mould growth and few in several other nations [7]. It is evident from the above literature study that research on mould growth in built environments is inferential and therefore insufficient to develop policies for a sustainable built environment in India.

Furthermore, these studies do not provide a numerical description of how many water stains, what level of visible mould growth, or how great a severity of musty odours are enough to warrant taking measures to offset detrimental health effects. This implies that there is still a lot to learn about the intricate link between mould growth on building materials and parameters, such as surface temperature and humidity; radiant temperature; ambient RH; DBT; wet-bulb temperature (WBT); wet-bulb depression (WBD); radiation; and so on, especially in the warm-humid climate of India. Additionally, energy-efficient building construction materials are being recommended without even understanding their mould resistance properties. Comfort and health-related standards for buildings do not stress averting, monitoring, and controlling excess moisture and dampness either inside or outside the building [7]. Keeping in mind the above background and research gap, this study aims at assessing the mould-growth index for exterior wall assembly that is made with inorganic capillary active-insulation material, i.e., AAC (autoclaved aerated concrete) brick-wall assembly without any moisture preventive coating, for a representative commercial building in the coastal city of Mangalore, Karnataka (KA), India, using the heat and mass transfer (HAMT) algorithm by integrating EnergyPlus through the Python plugin. Furthermore, this study will help study the parameters that are the key drivers that promote mould growth on a material.

2. Materials and Methods

The following section provides a step-by-step guide to the mould development study for Mangalore's warm and humid climate. For this study, one case is being used, and the details have been summarized in four parts, as follows.

2.1. Location and Energy Model Inputs

For this study, one case of a low-rise commercial building model in Mangalore, Karnataka, India, with a warm and humid climate has been used. The typical meteorological-year weather file for 2007–2021 from the Mangalore airport has been used for the weather input. The details have been derived from a reference model, introduced in [48], and its characteristics have been summarized in Table 3. It is important to note here that the study that was conducted across India to develop a reference building model which studied about 75 low-rise commercial buildings reported that 200 mm-thick AAC wall with cement plaster on the inside and outside is the most common exterior wall assembly [48]. Another thing to note here is that the exterior wall assembly does not have any moisture preventive coating.

Table 3 is divided into five categories: form, envelope, loads, systems, and assumptions, and these data help us to create a reference-model building.

Table 3. Building design inputs [48].

Sr. no.	Item	Unit	Low Rise
1. Form			
1.0	Total floor area above basement	m ²	3127
1.1	Percent of conditioned area	%	74
1.2	The floor area of the basement	m ²	NA
1.3	The shape of the building	-	Rectangular
1.4	Aspect ratio	Long/short side	2.82
1.5	No. of floors above grade	Number	3
1.6	The floor area above the grade	m ²	1042
1.7	No. of the floor below grade	Number	NA
1.8	Floor area below grade	m ²	NA
1.9	WWR (window-to-wall ratio)	%	30%
1.10	Geometry of the window shading	-	None
1.11	Room height (floor to floor)	m	3.96
1.12	Room height (floor to ceiling)	m	3.05
1.13	Sill height of the window	m	0.92
2. Envelope			
2.0	Exterior wall construction—warm-humid	Description	10 mm cement plaster + 200 mm AAC block + 10 mm cement plaster (from out to in) (No moisture preventive coating)
2.1	Wall U-factor	(W/m ² ·K)	1.4
2.2	Roof construction—warm-humid climate	Description	Concrete (150 mm) + expanded polystyrene (thermocole) (EPS) 30 mm (from out to in)
2.3	U-factor for roof	(W/m ² ·K)	1.03
2.4	U-factor for window	(W/m ² ·K)	2.13
2.5	SHGC of window	-	0.25
2.6	Window VLT	%	37
3. Loads			
3.0	Average LPD—building area method	W/m ²	Basement parking: NA office space: 7.7
3.1	Daylight controls	-	None
3.2	Occupancy controls	-	None
3.3	Elevator	kW	12
3.4	Exterior lights	kW	3.6
3.5	Basement ventilation	kW	NA
4. Systems			
4.0	Cooling type	Description	VRF
4.1	Distribution and terminal units	Description	Ductable CAV AHU
4.2	COP	Unitless	3.49
4.3	Economisers	Description	NA
4.4	Demand control ventilation	Description	No
4.5	Energy recovery	Description	In fresh-air unit with 70% effectiveness
4.6	Supply fan power	Watt/lit/sec	0.64
4.7	Pump—chilled water configuration	-	NA
4.8	Pump—chilled water control	-	NA
4.9	Pump—chilled water power	Watt/lit/sec	NA
4.10	Pump—chilled water head	m	NA
4.11	Pump—condenser water control	-	NA
4.12	Pump—condenser water power	Watt/lit/sec	NA
4.13	Pump—condenser water head	m	NA

Table 3. Cont.

Sr. no.	Item	Unit	Low Rise
4.14	Water volume	lit	NA
4.15	Type	-	NA
4.16	Performance	lit/sec/kW	NA
4.17	Fan type	-	NA
4.18	Fan control	-	NA
5. Assumptions			
5.0	Occupancy	m ² /person	14
5.1	Ventilation	Lit/sec·m ²	2.5 + 0.3
5.2	Thermostat set point	-	25 °C cooling/20 °C heating
5.3	Thermostat set-back	-	30 °C cooling/15 °C heating
5.4	Window locations	-	Even distribution among all four sides
5.5	Azimuth	-	Non-directional
5.6	Window dimensions	-	Based on window fraction, location, glazing sill height, floor area, and aspect ratio
5.7	Infiltration	-	Peak: 0.0010 m ³ /sec·m ² of above-grade exterior wall surface area (when fans turn off) Off-peak: 25% of peak infiltration rate (when fans turn on)
5.8	Plug load	W/m ²	16.14
5.9	Supply air temperature	-	Temperature difference of 11 °C for supply-air-to-room-air

Based on the inputs, a 5-zone model with a core-perimeter zone has been developed, with the perimeter zone kept at 5 m, as per ECBC 2017 recommendations. Figure 4 shows the geometry of the building [49].

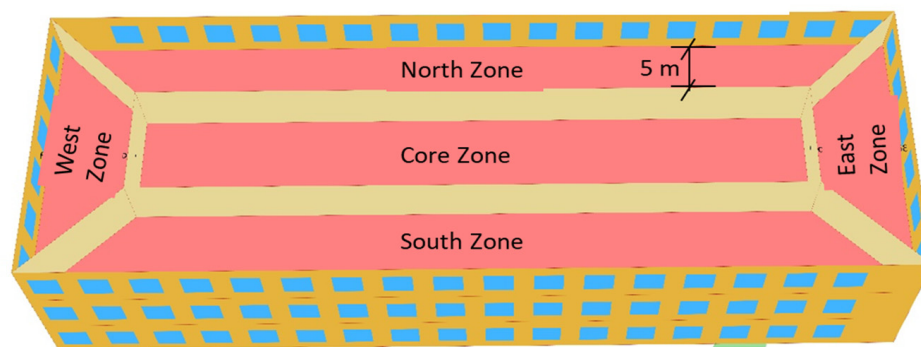


Figure 4. ECBC model building showing the 5 thermal zones, i.e., north zone, south zone, east zone, west zone, and core zone. The perimeter zone is kept at 5 m.

2.2. Hygrothermal Properties of Materials for Heat and Mass Transfer (HAMT)

The HAMT extension for EnergyPlus has been considered for mould-growth simulation. HAMT, in combination with EnergyPlus, is a heat and moisture transfer model that simulates the simultaneous transport and storage of heat and moisture in surfaces from and to both internal and external environments. Its transient energy modelling capabilities assist in simulating moisture-buffering effects, providing temperature and moisture profiles through composite building walls, and identifying regions with high surface humidity [30,50]. The hygroscopic sorption properties for the AAC blocks and cement mortar have been identified in [51,52] and are summarized in Table 4.

Table 4. Hygrothermal properties of aerated concrete and cement (AAC) mortar [51,52].

Material name Porosity [m ³ /m ³] Initial water-content Ratio [kg/kg]		Aerated Concrete 0.7 0.0180				
RH fraction [–]	Moisture content [kg/kg]	Moisture content [kg/m ³]	Suction-liquid transport coefficient [m ² /s]	Redistribution- liquid transport coefficient [m ² /s]	Water vapour diffusion-resistance factor [–]	Thermal conductivity [W/m·K]
0					100	
0.178	0.0180	11.56	4.31×10^{-9}	4.31×10^{-9}		
0.331	0.0230	14.77				
0.548	0.0240	15.41				
0.557	0.0280	17.98				
0.753	0.0290	18.62				
0.763	0.0350	22.47				
0.903	0.0460	29.53				0.384
0.924	0.0640	41.09				
0.953	0.0910	58.42				
0.965	0.1000	64.20	2.00×10^{-9}	2.00×10^{-9}		0.479
0.980	0.1650	105.93				0.571
0.988	0.1850	118.77				0.643
	0.2200	141.24	6.67×10^{-9}	6.67×10^{-9}		
	0.3200	205.44	4.17×10^{-8}	4.17×10^{-8}		
	0.4200	269.64	4.17×10^{-8}	4.17×10^{-8}		
	0.5200	333.84	6.00×10^{-8}	6.00×10^{-8}		
	0.6200	398.04	2.00×10^{-8}	2.00×10^{-8}		
	0.7200	462.24	2.00×10^{-8}	2.00×10^{-8}		
	0.8200	526.44	4.79×10^{-8}	4.79×10^{-8}		
	0.9200	590.64	1.97×10^{-7}	1.97×10^{-7}	60	
Material name Porosity [m ³ /m ³] Initial water-content ratio [kg/kg]		Cement mortar 0.327 0.2				
Relative humidity fraction [–]	Moisture content [kg/kg]	Moisture content [kg/m ³]	Suction-liquid transport coefficient [m ² /s]	Redistribution- liquid transport coefficient [m ² /s]	Water vapour diffusion-resistance factor [–]	Thermal conductivity [W/m·K]
0	0	0				1.722
0.251	0.0117	3.25	2.00×10^{-9}	2.00×10^{-9}		1.942
0.254	0.0126	3.50				
0.445	0.0156	4.34				
0.451	0.0166	4.61				
0.648	0.0268	7.45				
0.652	0.0226	6.28	4.00×10^{-9}	4.00×10^{-9}		2.092
0.847	0.0328	9.12	5.60×10^{-9}	5.60×10^{-9}		2.172
0.854	0.0330	9.17				
0.952	0.0461	12.82				
0.956	0.0467	12.98				
0.976	0.0538	14.96	1.40×10^{-8}	1.40×10^{-8}		2.282
0.977	0.0548	15.23	1.00×10^{-8}	1.00×10^{-8}		
	0.0600	16.68	2.00×10^{-8}	2.00×10^{-8}		2.322
	0.0700	19.46				2.372
	0.0760	21.13	1.70×10^{-8}	1.70×10^{-8}		
	0.0840	23.35	3.20×10^{-8}	3.20×10^{-8}		
	0.0900	25.02	6.80×10^{-8}	6.80×10^{-8}		

2.3. Mould-Growth Index Model—ASHRAE and EnergyPlus

Various mathematical approaches to calculate the MGI for building materials have been investigated in the past. However, it appears that the performance assessment methods for mould growth are overly strict. For the purpose of this study, we have used a mathematical model and equations, as specified in ASHRAE 160-2016. Prior to simulations, it is essential to identify the sensitivity class for the material under study, i.e., classified between very sensitive, sensitive, medium-resistant, or resistant. The mould index (M) is set at zero at the initial setting ($M = 0$ at time $t = 0$) and can be calculated for each hour using Equation (3).

$$M_t = M_{t-1} + \Delta M \quad (3)$$

where M_t is the current-hour mould index; M_{t-1} is the previous-hour mould index; and ΔM is the change in the mould index, calculated for each hour as specified in ASHRAE 160-2016. It is suggested that the mould index must have a minimum value of zero. If $M_{t-1} + \Delta M$ produces a negative number at any time step, M_t must be set to zero at that time

step. If the current hour's surface temperature (T_s) is more than 0°C , the critical-surface relative humidity for mould initiation (RH_{crit}) must be computed using the equation in ASHRAE 160-2016. Equation (4) is to be used for a material which falls under a very sensitive or sensitive class. Equation (5) is to be used for a material which falls under a medium-resistant or resistant class.

$$\text{RH}_{\text{crit}} = -0.00267 T_s^3 + 0.160 T_s^2 - 3.13 T_s + 100 \text{ when } T_s \leq 20^\circ\text{C}, 80 \text{ when } T_s > 20^\circ\text{C} \quad (4)$$

$$\text{RH}_{\text{crit}} = -0.00267 T_s^3 + 0.160 T_s^2 - 3.13 T_s + 100 \text{ when } T_s \leq 7^\circ\text{C}, 85 \text{ when } T_s > 7^\circ\text{C} \quad (5)$$

Now, if the relative humidity at the material surface (RH_s) is larger than the RH_{crit} at the current hour, then an increase in the mould index must be calculated using Equation (6). Here, k_1 is the mould-growth intensity factor; k_2 is the mould-index attenuation factor, and W is the sensitivity class.

$$\Delta M = \frac{k_1 k_2}{168 \cdot \exp(-0.68 \ln T_s - 13.9 \ln \text{RH}_s + 0.14W + 66.02)} \quad (6)$$

Furthermore, the mould-index attenuation factor (k_2) can be calculated using Equation (7). The M_{max} in Equation (7) is the maximum mould index corresponding to the surface temperature and relative humidity at the current hour, which is calculated using Equation (8).

$$K_2 = \max \{1 - \exp[2.3 (M - M_{\text{max}})], 0\} \quad (7)$$

$$M_{\text{max}} = A + B \left(\frac{\text{RH}_{\text{crit}} - \text{RH}_s}{\text{RH}_{\text{crit}} - 100} \right) - \left(\frac{\text{RH}_{\text{crit}} - \text{RH}_s}{\text{RH}_{\text{crit}} - 100} \right)^2 \quad (8)$$

where A , B , and C are the coefficients reflecting the material sensitivity class [13].

2.4. Flowchart of the Process

For this study, mould growth was studied in an AAC block wall assembly in the warm and humid climate of Mangalore. This starts with identifying representative commercial buildings' geometry, envelope, and usage profiles for the Indian context; the database for hygro-thermal properties also needs to be identified. An EnergyPlus model for HAMT simulation was developed based on the above information. The EnergyPlus simulation generated hourly indoor and outdoor surface temperature and surface humidity results. The script for the EnergyPlus Python plugin to calculate the MGI was developed, and key variables responsible for mould growth were identified. The process is presented in Figure 5.

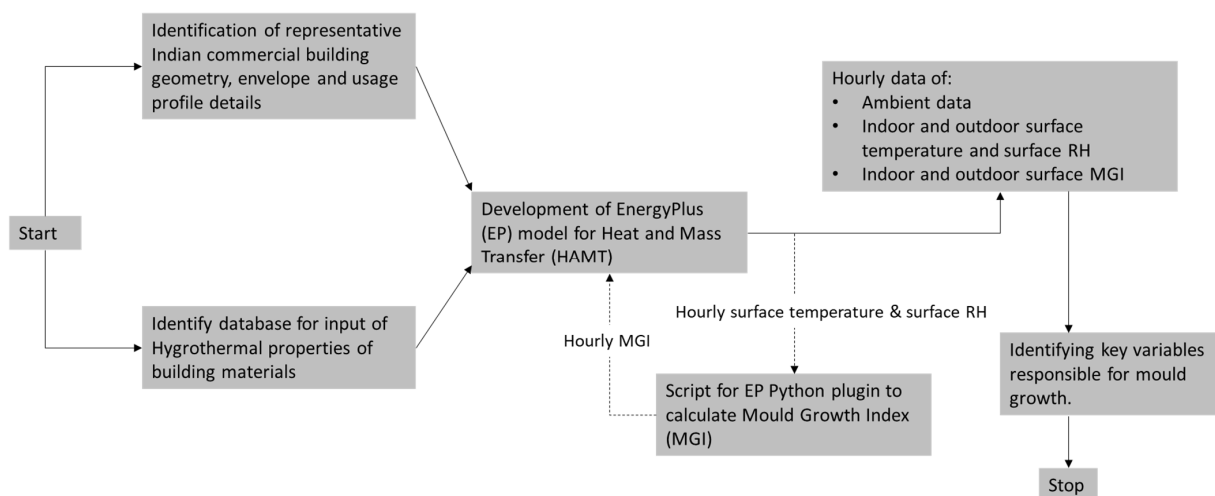


Figure 5. Flowchart for the HAMT simulation.

3. Results and Discussion

The following section summarizes the results for the MGI. As EnergyPlus is built on the fundamentals of building heat transfer and loads simulation, any flaws in the load calculation will inevitably lead to inaccuracies in the heating, ventilation, and air-conditioning (HVAC) calculations of comparable or greater scale. It is unclear how much error would be introduced into the outcomes in the supposedly rare circumstance where convergence is not achieved before the simulation begins. While annual simulations should balance out any initial condition issues by the sheer number of days in the simulation, design day simulations, especially those that are used for HVAC system sizing, could result in severe inaccuracies. For this purpose, the results and findings are divided into three sections, i.e., the climate profile of Mangalore, convergence cases and statistical analysis, and MGI results and correlations.

Furthermore, for this HAMT simulation, we have considered warm-up days of 1, 6, 12, 25, 50, and 100 days. It is important to identify the error in the results of MGI calculation, and this can be achieved by identifying the appropriate warm-up days for the calculation of MGI. When steady periodic circumstances are not achieved, simulation results may be erroneous. As a result, it is critical to know when there are enough historical data on temperature and flux to start an EnergyPlus simulation, as this has the potential to have an economic and energy impact on buildings that employ EnergyPlus in design [53].

For ease of understanding, we have calculated MGI for the south façade of the building and shown its relationship with the outside surface temperature and outside surface relative humidity. The results suggest that required convergence is achieved when warm-up days are kept at 25 days, beyond which the model tends to over-predict the MGI. It is observed that the higher the convergence values, the higher the MGI. Moreover, the slope pattern and spread of MGI, the surface temperature and the surface humidity were found to be similar for all convergence scenarios. In higher convergence scenarios, we observe that the minimum MGI starts from 4, while for lower convergence, the minimum MGI starts from 0. With a higher number of convergences runs, the initial moisture content becomes rather high, which usually does not occur in new buildings.

3.1. Climate Profile of Mangalore

The coastal city of Mangalore has a warm and humid climate, as per ECBC 2017, and is located at 12.91° N and 74.85° E latitude and longitude, respectively. This port city is situated in the southwest of India in the state of Karnataka, on the coast of the Arabian Sea, and it lies in between the Gurupura and Netravati rivers, whose confluence is near the coast. To the east of the city lies the Western Ghats.

The DBT across the year ranges from 22.0 to 34.0 °C, with the maximum temperature reached during the afternoon hours from January to April and October to December, as demonstrated in Figure 6.

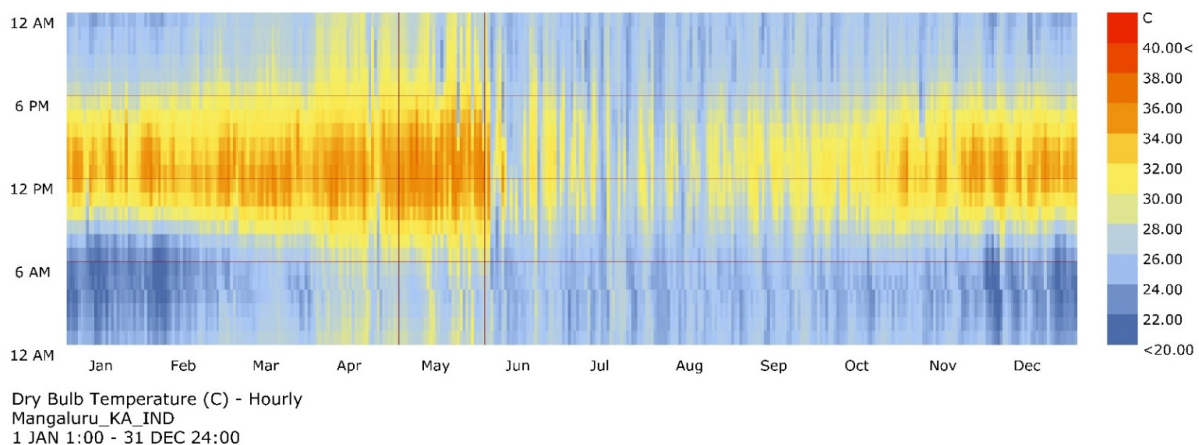


Figure 6. Dry-bulb temperature for the Mangalore city. (Source: authors.)

The dew-point temperature (DPT) ranges from 20.0 to 30.0 °C across the year, with an average annual wet-bulb depression of 4.5 °C. It is important to understand that the DPT as the concept of humidity comfort level is based on the dew point. Moreover, DPT impacts the moisture content and the water activity on the material surface. Lower DPT means dry ambient conditions and higher DPT means more humid conditions. It is important to remember that DPT is independent of the ambient temperature. Unlike DBT, which naturally varies significantly between night and day, DPT tends to vary gradually. This means that if the DPT is high during the daytime, the night-time DPT will also be similar, and hence cause continuous exposure to ambient humid conditions on the building material surface. Mangalore experiences significant seasonal variation in the perceived humidity. In Figure 7, it can be seen that from January to December, the DPT range of 20.0–28.0 °C is prevalent for at least 75–80% of the time. According to ASHRAE standard 55-2017, the ideal dew-point temperature is about 16.0–17.0 °C.

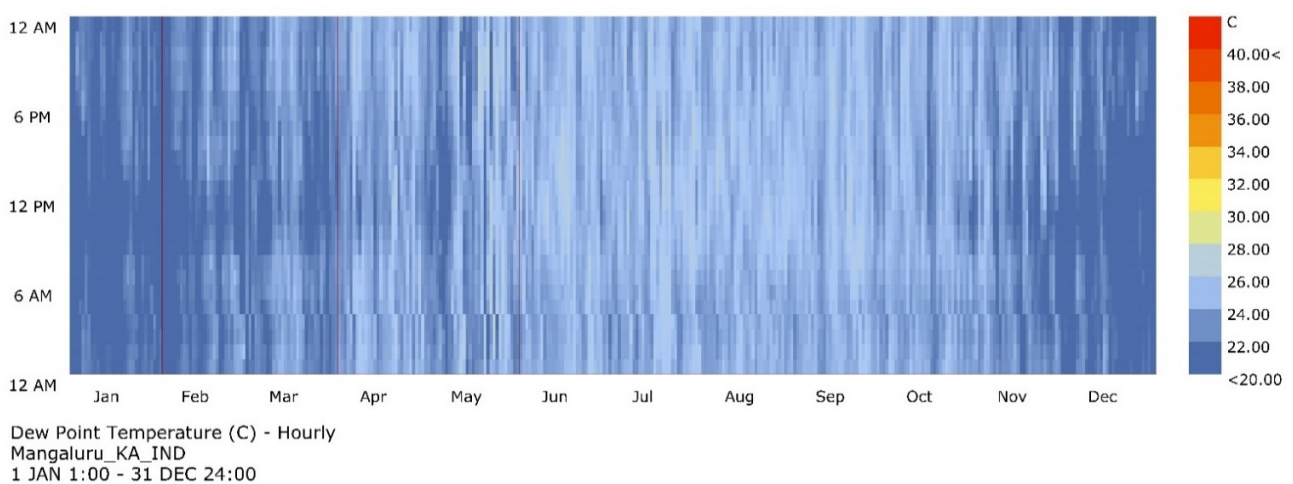


Figure 7. Dew-point temperature for the Mangalore city. (Source: authors).

Mangalore receives an annual average of 3479 mm of precipitation, which makes it the second-highest receiver of rainfall in India. February could be identified as the driest month of the year, receiving about 2 mm of rain, followed by January (4 mm), March (17 mm), and December (19 mm). On the other hand, July could be identified as the wettest month, receiving about 1059 mm of rainfall, followed by August (704 mm). The annual average RH is 77.5%, with a maximum of 94% from June to October and a minimum of 41% during January and February, as seen in Figure 8.

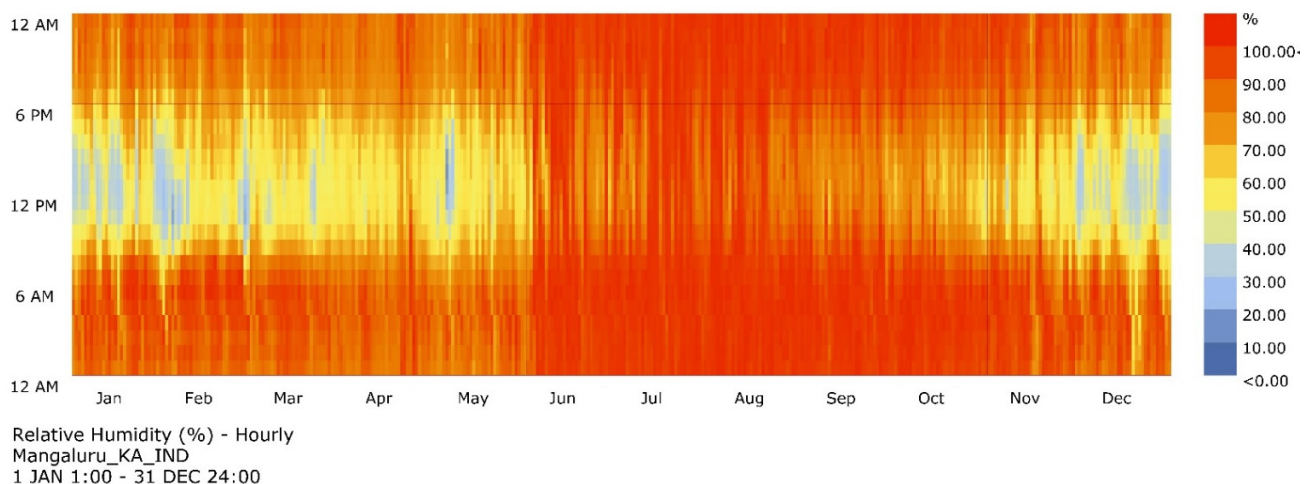


Figure 8. Relative humidity for Mangalore city. (Source: authors).

Mangalore, being close to the equator, is expected to receive maximum radiation, although due to its proximity to the coast and the equator, it has high cloud cover throughout the year. There are about 3234 h of sunshine across the year in Mangalore. The annual average direct normal solar radiation is 414 Wh/m², with the maximum reaching up to 829 Wh/m² in January and February, whereas the minimum is noted at 47 Wh/m² during the monsoon months from June to September, as seen in Figure 9.

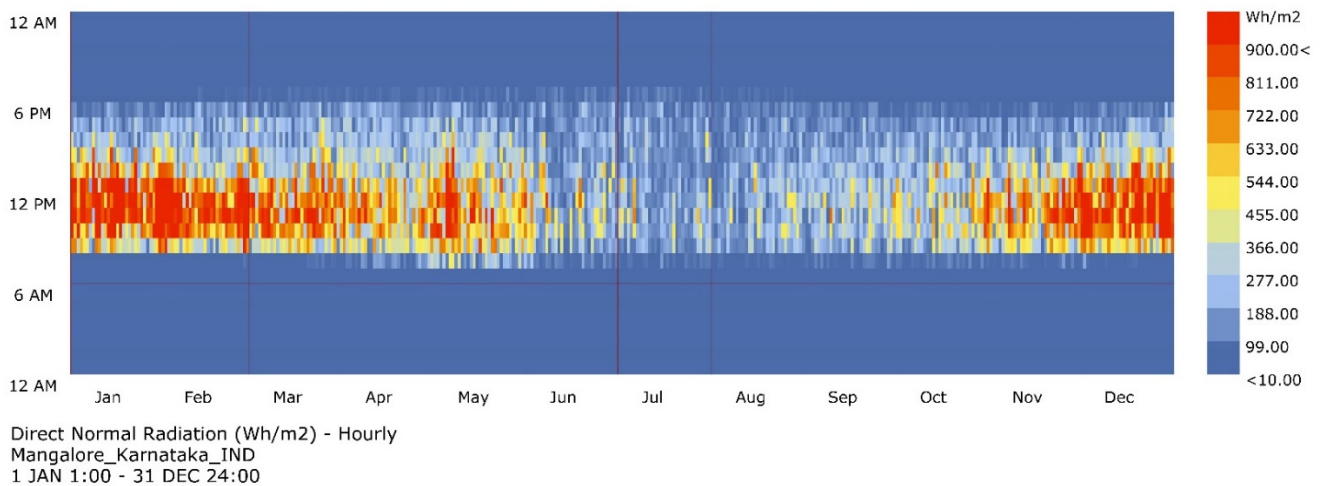


Figure 9. Direct normal solar radiation for Mangalore city. (Source: authors).

It can be understood from the climate analysis that Mangalore has a warm-humid climate, and the temperature and humidity conditions are such that they can promote mould growth.

3.2. Convergence Cases and Statistical Analysis

EnergyPlus, by default, sets the surface temperatures of each new environment to 23 °C, and the zone humidity ratios to the outdoor humidity ratio. The environment's first-day conditions are iterated until the loads/temperature convergence tolerance values given in the building object are satisfied, or the "maximum number of warm-up days" is reached. If enough temperature and flux history loads are not achieved during these periodic steady conditions the simulation results may be erroneous. For this purpose, the authors have identified and simulated six convergences to understand the impact of changing the number of warm-up days. They are summarized in Table 5.

Table 5. Convergence cases with minimum and maximum warm-up days. (Source: authors.)

Convergence Cases	Min Warm-Up Days	Max Warm-Up Days
Con 01	1	1
Con 06	1	6
Con 12	1	12
Con 25	1	25
Con 50	1	50
Con 100	1	100

Furthermore, the R² correlation between surface temperature and surface humidity, and maximum MGI and minimum MGI have been studied for the inside and outside surfaces of the AAC wall construction. R-squared is a goodness-of-fit indicator for a linear regression model. The R-squared value suggests the percentage of the variance in the dependent variable that the independent variables explain collectively. R-squared varies between 0 and 1, where 1 suggests a strong correlation between the parameters. The results are summarized in Figure 10, Tables 6–8.

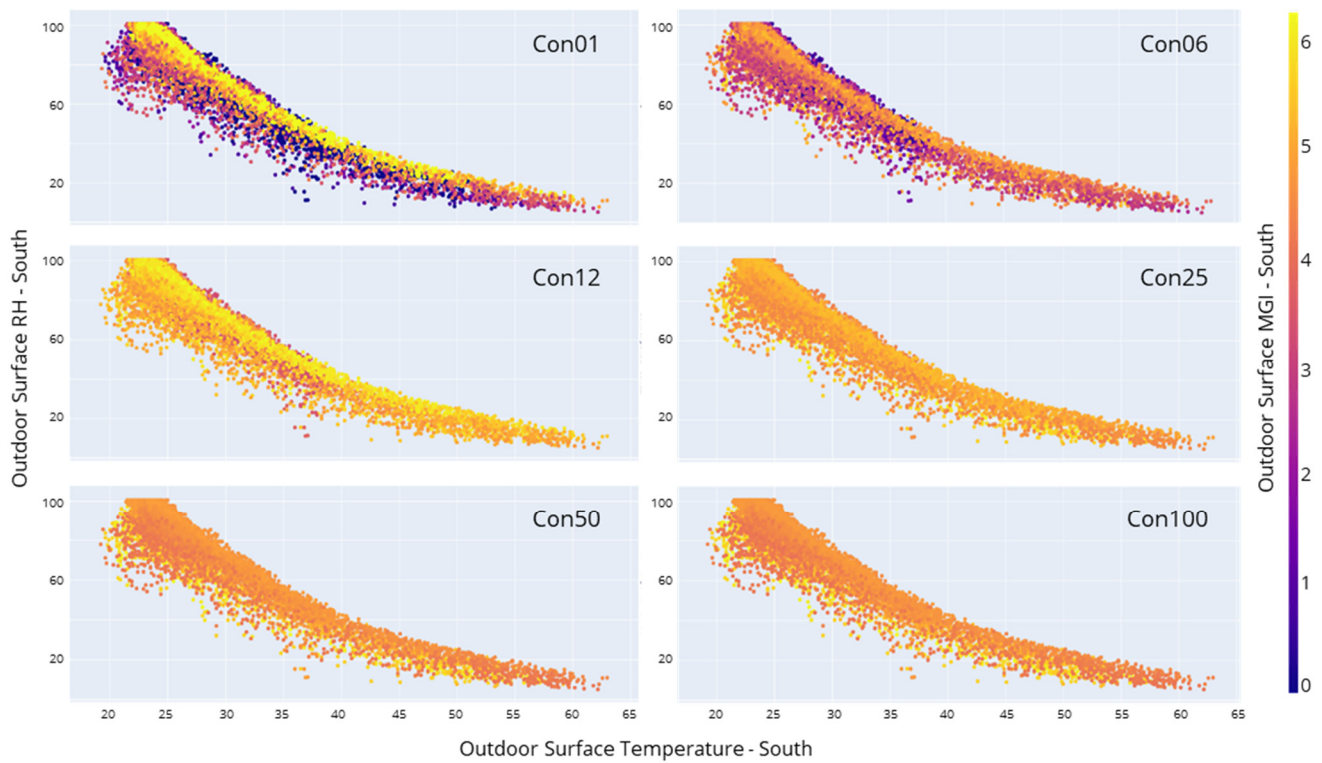


Figure 10. MGI in relation to DBT and RH for Con01, Con06, Con12, Con25, Con50, and Con100. (Source: authors.)

Table 6. R² value and correlation between surface temperature and surface humidity for the AAC wall assembly. (Source: authors.)

Convergence Cases	Inside Surface				Outside Surface			
	North	East	South	West	North	East	South	West
Con 01	0.57	0.69	0.67	1	0.89	0.94	0.94	0.93
Con 06	0.58	0.69	0.68	1	0.89	0.94	0.94	0.93
Con 12	0.57	0.69	0.67	1	0.89	0.94	0.94	0.93
Con 25	0.57	0.69	0.67	1	0.89	0.94	0.94	0.93
Con 50	0.57	0.69	0.67	1	0.89	0.94	0.94	0.93
Con 100	0.57	0.69	0.67	1	0.89	0.94	0.94	0.93

Table 7. R² value and correlation for maximum MGI for AAC wall assembly. (Source: authors.)

Convergence Cases	Inside Surface				Outside Surface			
	North	East	South	West	North	East	South	West
Con 01	0.18	0.17	0.18	0.19	0.61	0.42	0.95	0.39
Con 06	0.44	0.45	0.43	0.46	1.08	0.98	1.25	1.04
Con 12	0.78	0.83	0.78	0.87	2.17	2.03	2.46	2.11
Con 25	1.49	1.61	1.49	1.71	3.86	3.67	4.2	3.75
Con 50	1.86	2.05	1.86	2.18	6	5.92	6	5.98
Con 100	1.93	2.13	1.93	2.27	6	6	6	6

It was observed that Con01, Con06, and Con12 cases tend to underpredict mould growth, whereas Con50 and Con100 cases tend to overpredict the value of the mould-growth index. It was also identified that Con50 and Con100 cases could be used in an MGI study for existing and aged buildings. Furthermore, different warm-up days can be used depending on the building’s age and degree of deterioration to accurately model the existing buildings. Additionally, it was also observed that the time taken to complete the computation by software increased by increasing the maximum warm-up days.

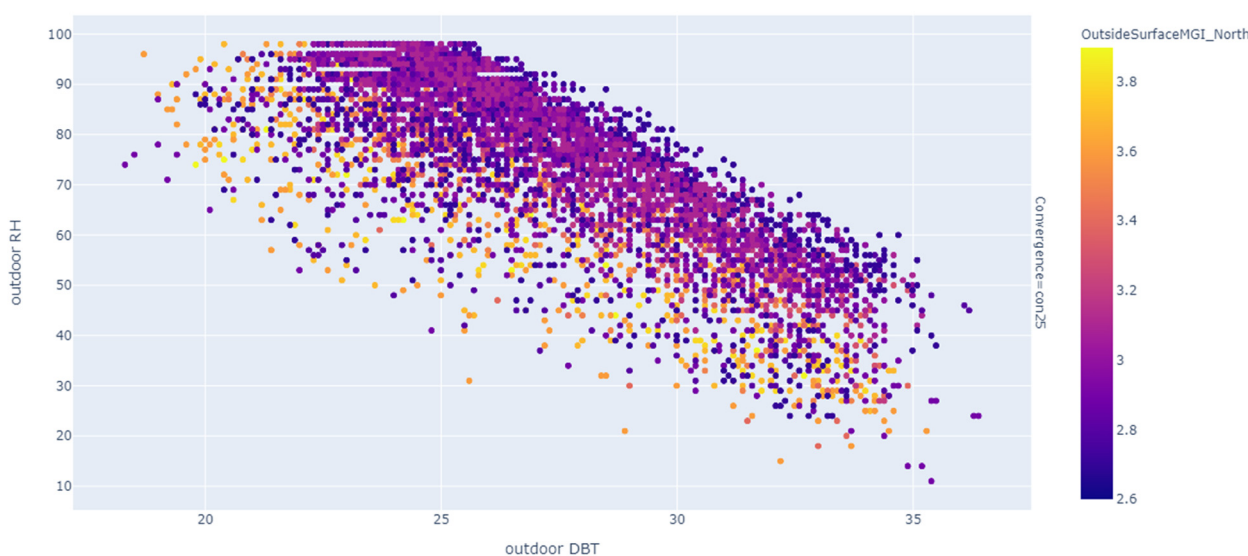
Table 8. R^2 value and correlation for minimum MGI for the AAC wall assembly. (Source: authors.)

Convergence Cases	Inside Surface				Outside Surface			
	North	East	South	West	North	East	South	West
Con 01	0	0	0	0	0	0	0	0
Con 06	0	0	0	0	0	0	0	0
Con 12	0	0	0	0	1.13	0.86	1.28	0.96
Con 25	0	0	0	0	2.64	2.23	2.84	2.23
Con 50	0	0	0	0	3.88	3.63	4.06	3.58
Con 100	0	0	0	0	3.98	3.79	4.1	3.72

It was observed that the correlation value for all the cases remained the same. However, the minimum and maximum values of MGI shift from lower to higher ranges from Con06 to Con100. For the Con25 case, an MGI of 4 to 6 has been calculated on the southside of the AAC wall assembly when the surface temperature and relative humidity are 25–30 °C and 60–100% RH, respectively, as shown in Figure 10. These results are in line with the maximum possible MGI that was noted in the literature review. This suggests that the simulation is running as it should. This research has also indicated that the default value of 25 warm-up days should be used, as it gives the most reliable results for newly constructed buildings. Additionally, similar representations have been made for the east, west and north side, and the results show a similar correlation for all the convergence cases between outdoor surface temperature and outdoor surface relative humidity.

3.3. MGI Results and Correlations

This section discusses MGI on the outside surface for the AAC wall assembly with outdoor RH and outdoor DBT. The MGI results for all four orientations are discussed. It can be observed from Figure 11 that the north side with an AAC wall assembly has an MGI ranging from 2.6 to 3.8 when the outdoor DBT and outdoor RH are in the range of 20 °C–33 °C and 60–100%, respectively. It can be observed that even at a temperature above 35 °C and with an RH less than 20%, an MGI of 2.6 is reported. The accumulation of moisture in the material and mould growth is triggered when the outdoor DBT and RH are relatively low.

**Figure 11.** A correlation plot between MGI, outdoor DBT, and RH for the north wall with AAC wall assembly. (Source: authors.)

It can be observed from Figure 12 that the southside AAC wall assembly has an MGI ranging from 2.8 to 4.2 when the DBT and outdoor RH are in the range of 20–30 °C and 60–100%, respectively. It is important to note that the southside is at the most risk of mould

growth as compared to any other surface. The south side would receive enough radiation across the day and obtain enough nutrients for the mould to grow.

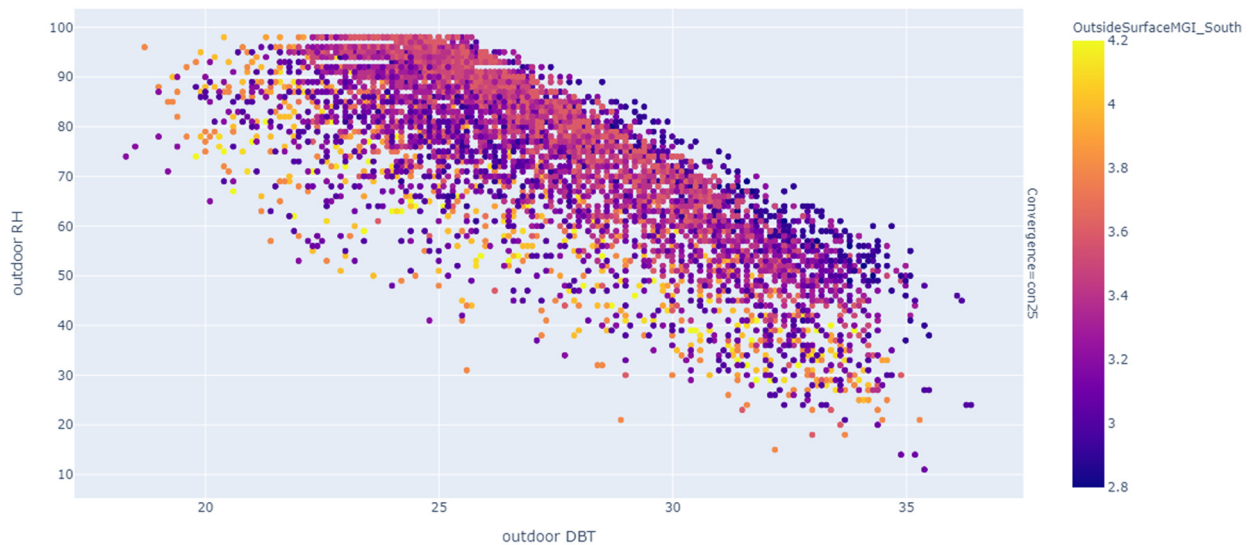


Figure 12. A correlation plot between MGI, outdoor DBT, and RH for the south wall with AAC wall assembly. (Source: authors.)

Figure 13 shows that the east side of the building with AAC wall assembly has an MGI ranging from 2.2 to 3.6 when the outdoor DBT and outdoor RH are in the range of 20–30 °C and 60–100%, respectively. It can be observed that the east wall has 14% less mould growth as compared to the south wall.

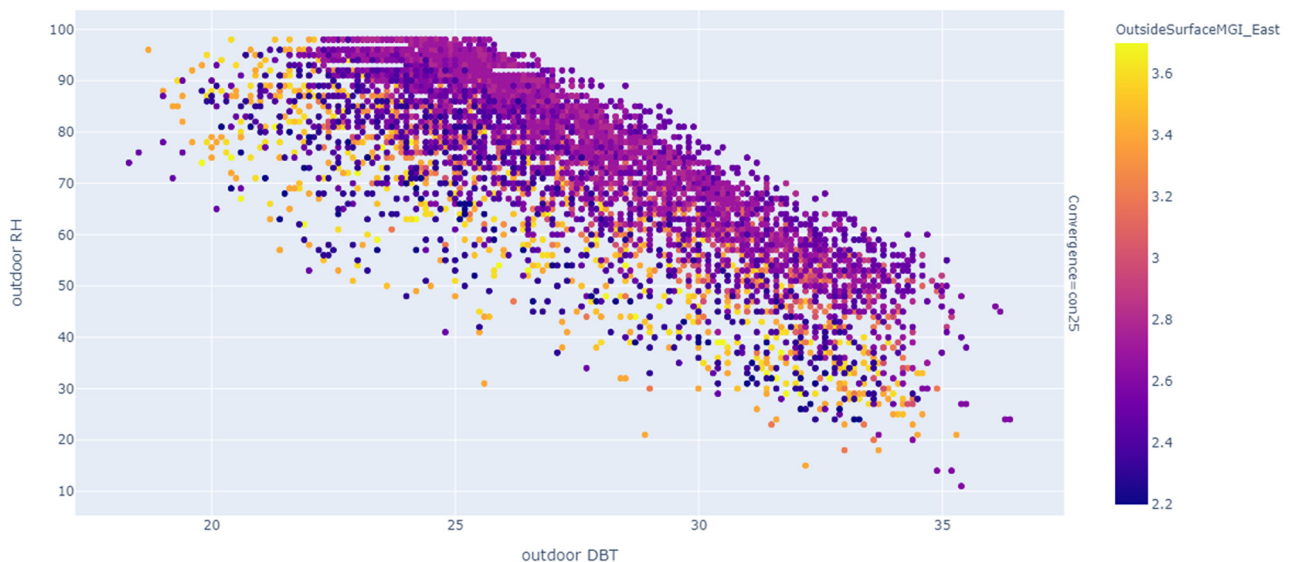


Figure 13. A correlation plot between MGI, outdoor DBT, and RH for the east wall with AAC wall assembly. (Source: authors.)

On the other hand, Figure 14 indicates that the west side with AAC wall assembly has an MGI ranging from 2.2 to 3.8 when the outdoor DBT and outdoor RH are in the range of 25–30 °C and 60–100%, respectively. This is 9.5% less as compared to the south side mould growth.

Furthermore, MGI has been plotted for all the orientations across the average year, as shown in Figure 15. It has been observed that the maximum mould growth is observed on the south side, followed by the north, west, and east facades across the year. The average annual mould growth ranges from 2.5 to 4.0, with MGI rising during the monsoon

months, i.e., June to October. The peak MGI is observed in October when there is limited precipitation, because the material continuously absorbs the water during the monsoon period. When there is high temperature and low humidity, mould growth is triggered, as these are favourable conditions. However, even during the driest month of the year, the average MGI does not fall below 2.5. This implies that the constituent materials that are used in the AAC wall assembly play an important role in causing mould growth. Further, once the mould growth is initiated, reversing it might prove to be very difficult. It is inevitable that material will have higher mould growth every subsequent year.

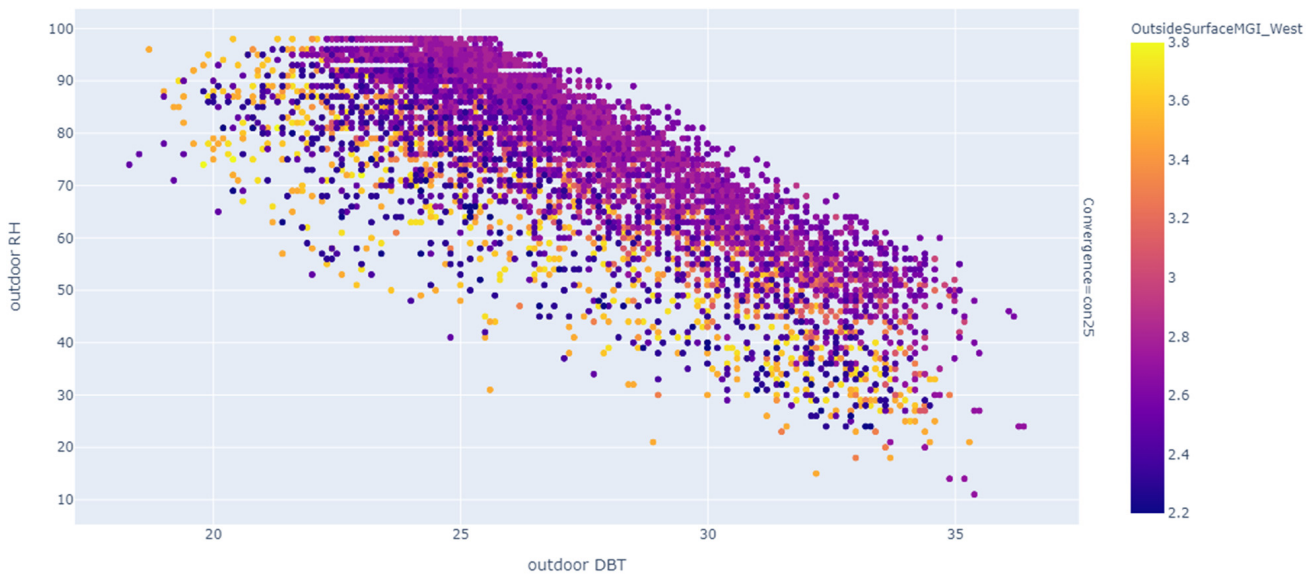


Figure 14. A correlation plot between MGI, outdoor DBT, and RH for the west wall with AAC wall assembly. (Source: authors.)

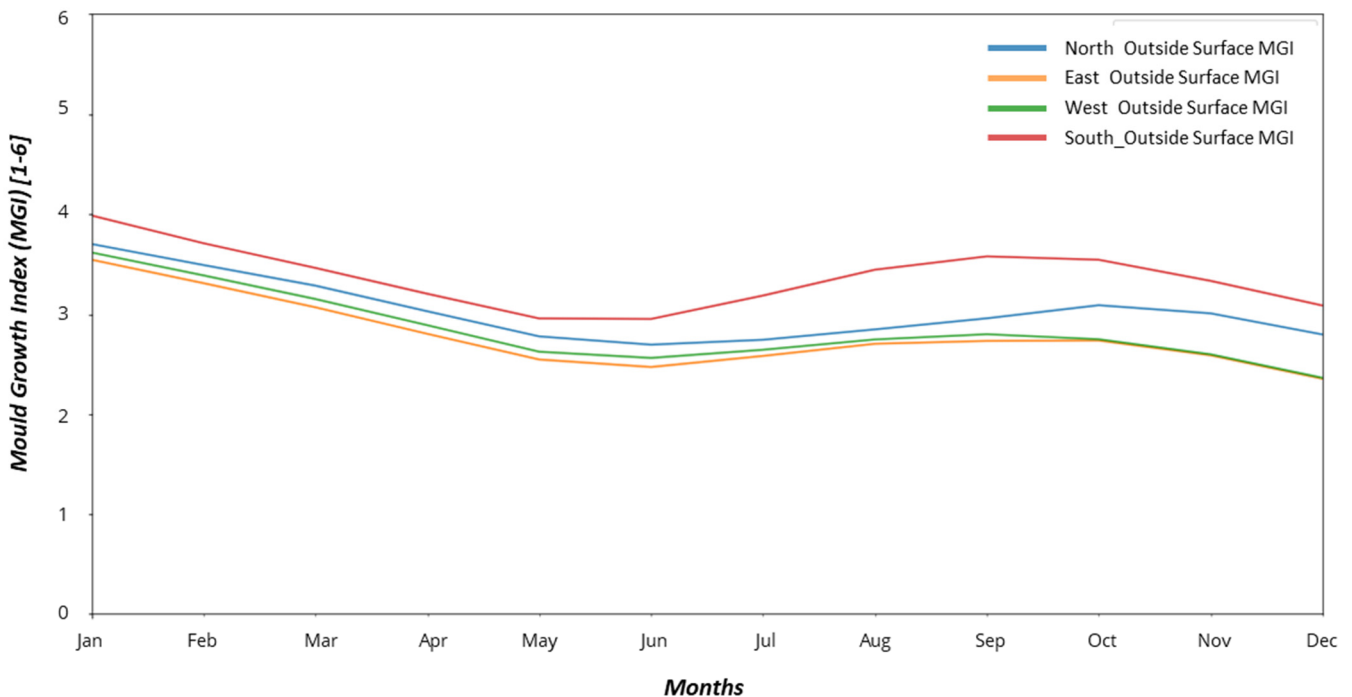


Figure 15. MGI profiles for the AAC wall assembly across the year for the four orientations, i.e., north, east, west, and south. (Source: authors.)

To understand the growth patterns of MGI across the months, a box plot was used. Based on Figures 16–19, the maximum mould growth with an MGI of 4.2 is observed from January to April and October to November in Mangalore for the south orientation. This is because global solar radiation and temperature are high in the range of 5.5 to 7.5 kWh/m² per day and 25–35°C on average, respectively, during May. Moreover, the moisture starts to seep into the material when it undergoes prolonged exposure to low ambient temperature and high ambient RH which is conducive to mould growth.

From the following Figure 16 (box plot of monthly MGI on the north orientation), a minimum MGI of 2.5 is observed in May and a maximum MGI between 3.0 to 4.0 is observed from January to April and October to November. It is interesting to note that the MGI reduces from January to April and rises again after the monsoon periods.

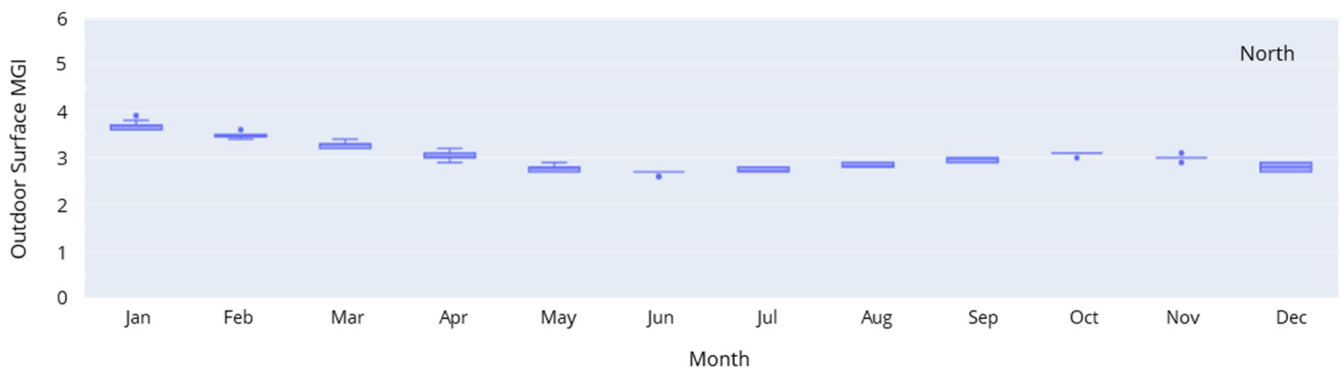


Figure 16. Box plot showing the monthly MGI results for the north wall. (Source: authors.)

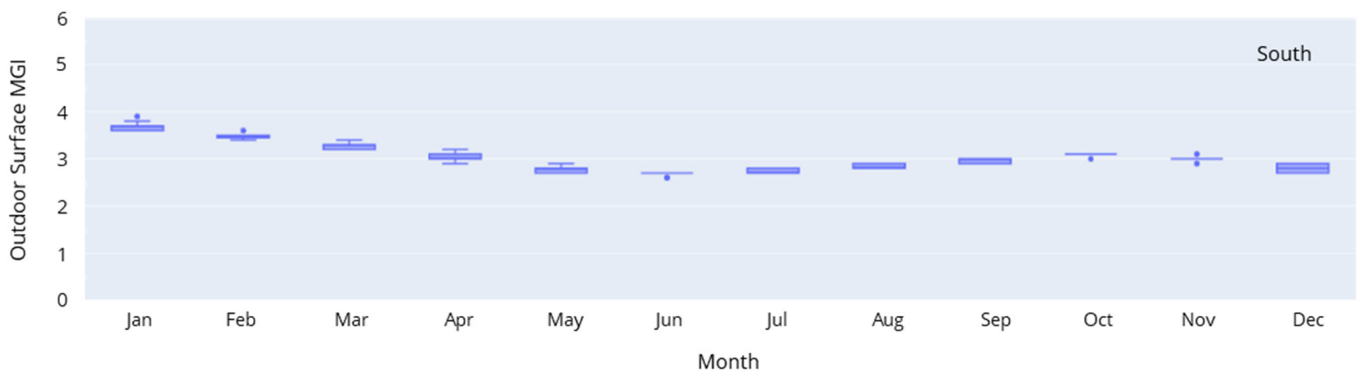


Figure 17. Box plot showing the monthly MGI results for the south wall. (Source: authors.)

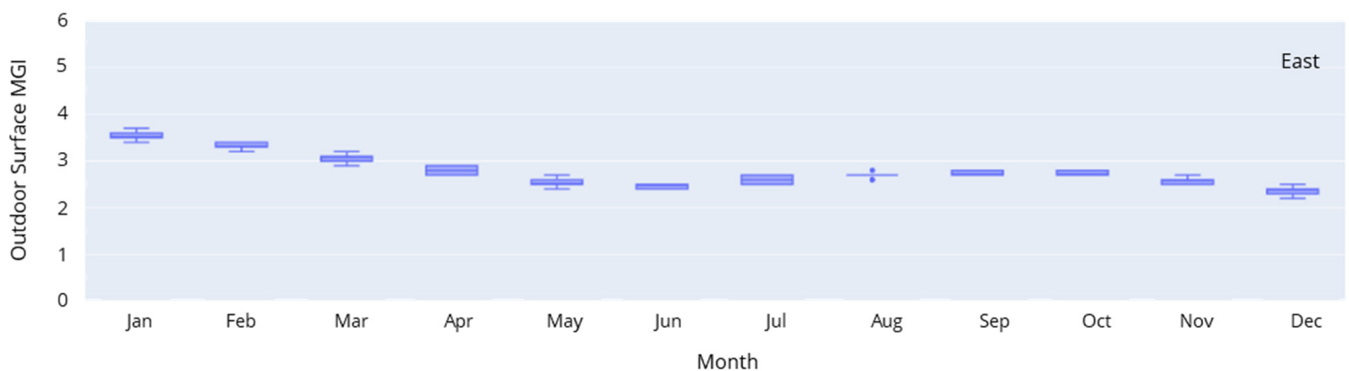


Figure 18. Box plot showing the monthly MGI results for the east wall. (Source: authors.)

From the box plot showing MGI on the south orientation (Figure 17), a minimum MGI of 2.8 is observed in May, and a maximum MGI of 3.0 to 4.2 is observed from January to April and October to November. It is worth noting that during September and October, the MGI is as high as 3.5 and the variation range is quite limited.

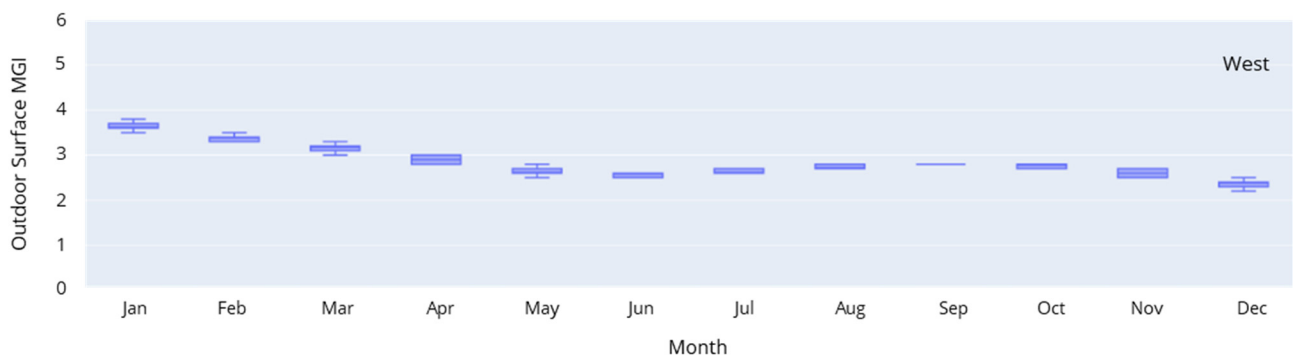


Figure 19. Box plot showing the monthly MGI results for the west wall. (Source: authors.)

From the box plot showing MGI on the east orientation (Figure 18), a minimum MGI of 2.5 is observed in May and a maximum MGI of 3.0 to 3.5 is observed from January to April. It is worth noting that the MGI on the east wall is below 3.0 for 75% of the year.

The box plot of the MGI on the west orientation (Figure 19) shows a minimum MGI of 2.2 in December and a maximum MGI of 3.0 to 3.5 from January to March. It is worth noting that the MGI on the west wall is below 3.0 for 75% of the year. However, the MGI is seen to rise during and after the monsoon season.

A parallel coordinates plot was also used, which allows a comparison between several individual parameters on a set of numeric variables, as shown in Figures 20–23. Each vertical bar represents a variable and often has a scale. Using Python, variables of outdoor DBT; RH; global horizontal radiation (GHR); direct normal radiation (DNR); diffuse horizontal radiation (DHR); outside surface temperature; and RH were plotted, with MGI values also plotted as a series of connecting lines across each axis. This provides a clear representation of all the values that are associated to each variable under all possible scenarios and helps to understand the major factor that impacts the MGI, as well as the probable months when mould will grow.

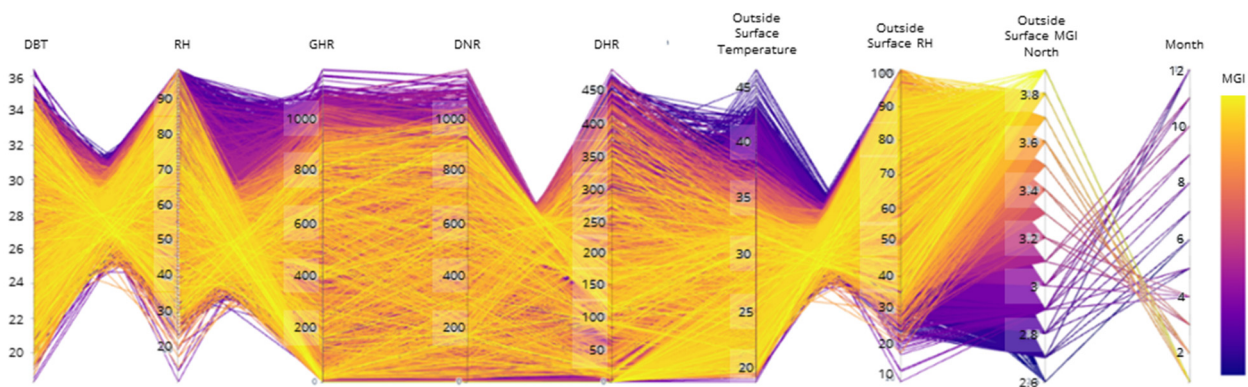


Figure 20. Parallel coordinates plot for the north side showing the relation between eight outdoor variables: dry-bulb temperature (DBT); relative humidity (RH); global horizontal radiation (GHR); direct normal radiation (DNR); diffuse horizontal radiation (DHR); outside surface temperature; outside surface relative humidity; and outside surface mould growth. (Source: authors.)

It can be seen in Figure 24 that the MGI in a commercial building in the Mangalore region ranges from 2.8 to 4.2. Additionally, surface temperature with surface RH of the material plays a very important role in the MGI. This is followed by outdoor DBT and RH, global horizontal radiation, as well as diffused horizontal radiation. It is important to note here that mould does not start to grow immediately as the DBT and RH conditions change, but after a few weeks of similar conditions. Furthermore, mould growth also depends on the material's water absorption and retention capacity.

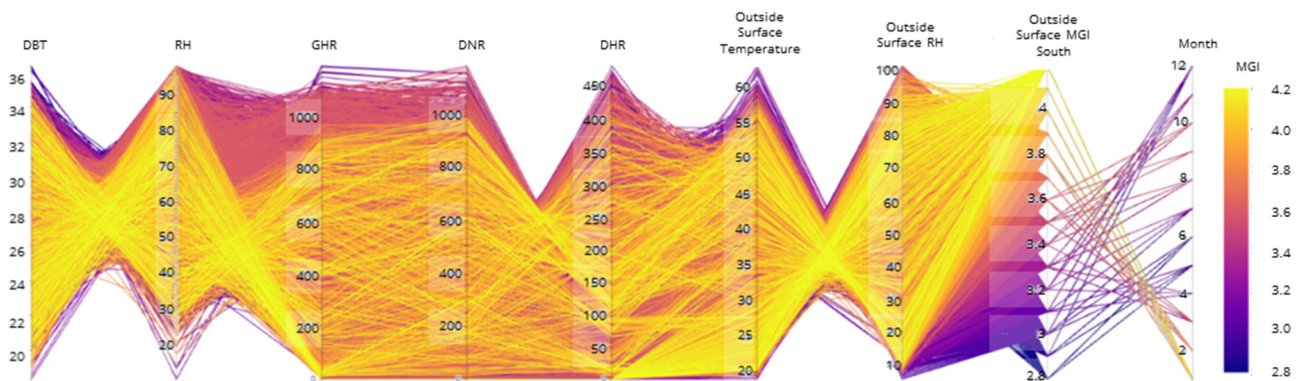


Figure 21. Parallel coordinates plot for the south side showing the relation between eight outdoor variables: dry-bulb temperature (DBT); relative humidity (RH); global horizontal radiation (GHR); direct normal radiation (DNR); diffuse horizontal radiation (DHR); outside surface temperature; outside surface relative humidity; and outside surface mould growth. (Source: authors.)

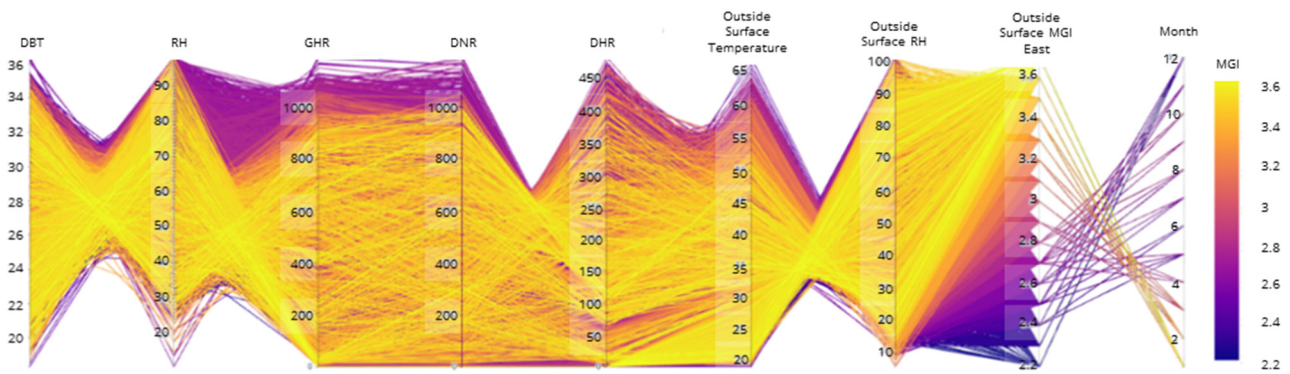


Figure 22. Parallel coordinates plot for the east side showing the relation between eight outdoor variables: dry-bulb temperature (DBT); relative humidity (RH); global horizontal radiation (GHR); direct normal radiation (DNR); diffuse horizontal radiation (DHR); outside surface temperature; outside surface relative humidity; and outside surface mould growth. (Source: authors.)

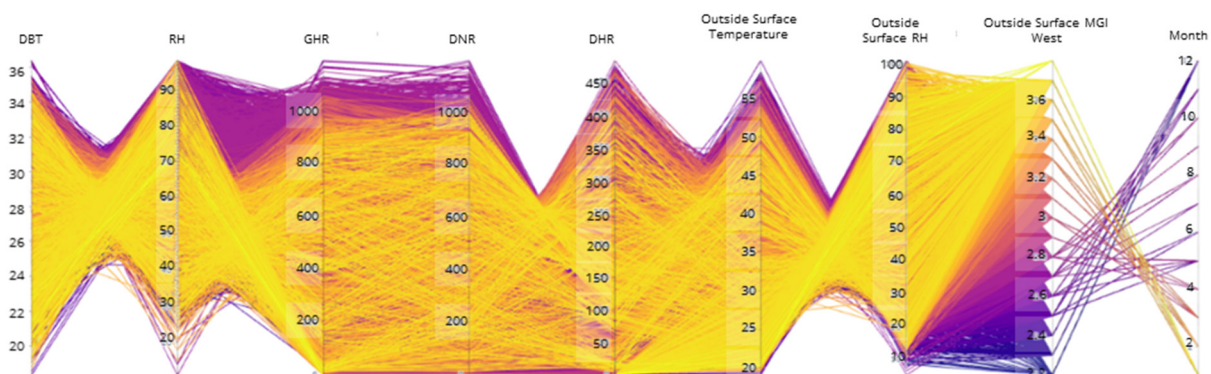


Figure 23. Parallel coordinates plot for the west side showing the relation between eight outdoor variables: dry-bulb temperature (DBT); relative humidity (RH); global horizontal radiation (GHR); direct normal radiation (DNR); diffuse horizontal radiation (DHR); outside surface temperature; outside surface relative humidity; and outside surface mould growth.

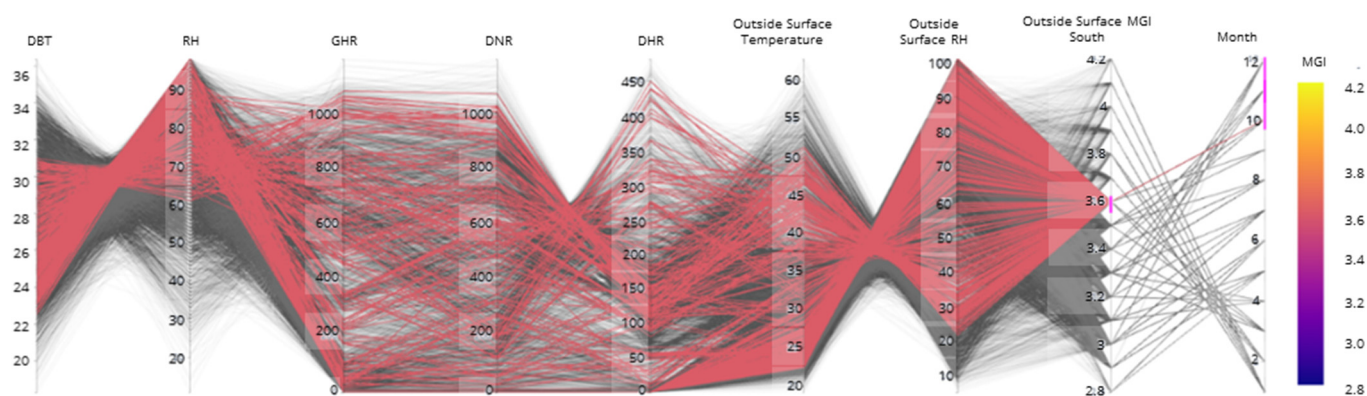


Figure 24. Parallel coordinates plot for the south side highlighting the parameters responsible for the MGI: dry-bulb temperature (DBT); relative humidity (RH); global horizontal radiation (GHR); direct normal radiation (DNR); diffuse horizontal radiation (DHR); outside surface temperature; outside surface relative humidity. (Source: authors.)

3.4. Discussion on Results Validation

To validate the results from this simulation study with real data, an experimental campaign has been designed to collect monitored data from a real building that was exposed to the same climatic conditions [54].

Our results suggest that in a coastal region, the annual mean MGI is 3.5, whereas a study that was conducted in a coastal climate region of Cornwall, South West England, using a temperature and RH sensor, and using the VTT mathematical model for mould growth, reported that MGI was in a range of 5.4 to 5.7 for non-wood materials, with a standard deviation ranging from 0.672 to 3.319 [55]. The same study also suggested that the critical RH of a material and the mouldy odour have a strong relationship with the mould growth on the material. These results are very much in line with our simulation study [55].

Comparative testing is another validation method [54] used by the authors where the outputs from EnergyPlus' HAMT are compared to WUFI's outputs. The results from a simulation study that was conducted in a coastal port city of Haikou, China, by using a bio-hygrothermal mould assessment model WUFI[®] Bio-simulation tool, and using the VTT mathematical model for MGI, was compared with the result from a simulation study that was conducted in the coastal port city of Mangalore, India. The results for the study that was conducted using WUFI in Haikou, China suggests that an AAC wall with a 0.357 mm thickness, a U-value of 1.13 W/m²·K, and an outside RH of 67–73% reports a mean MGI of 0.02 and a mould growth rate of less than 50 mm per year for a period of five years [56], whereas our study suggests a mean MGI of 3.5 for a period of one year. The reason behind such a wide difference might be because HAMT does not consider surface water absorption or precipitation. Rainwater leakage is another major cause of moisture-durability failure in building components. Additionally, it is also known that WUFI does not account for the exchange of heat and moisture at the interior and exterior boundary surfaces. It is also important to note that the EnergyPlus' HAMT model can be improved by adding one layer that will actively exchange moisture between the outdoors and other building layers [30]. In the current study, a 220 mm thick wall assembly has been considered with a total of three layers, as this method allows EnergyPlus to consider the moisture-based interaction with the outdoor climate (i.e., OUT to IN—10 mm cement plaster + 200 mm AAC wall + 10 mm cement plaster). Another study that was conducted using WUFI in Seoul, South Korea, reported that for exterior wall materials such as oriented strand board (OSB—12 mm thick) and glass wool (159 mm thick), the mean annual MGI is 2.36 whereas the mould growth rate is 195 mm per year [57]. The same study also reports that mould growth is higher on the exterior wall rather than the interior of the wall. The study also confirms that the water content and surface relative humidity are the key drivers responsible for the mould growth on a building material [57].

4. Conclusions

This paper summarizes the method and process to be followed for modelling mould growth in building envelopes using HAMT in the EnergyPlus engine. The mould growth on a building has been attributed to outdoor DBT and RH, although this is only partially true. This research has identified that the outdoor surface temperature and RH, along with the hygrothermal property of a material, play a crucial role in mould growth on the material. Additionally, radiation falling on each surface and the time for which the moisture exists on a material's surface also play an important role in mould growth. The annual mean MGI for the AAC assembly is 3.5, which suggests that mould growth is visible and will cover about 30–70% of the surface area. These results are only applicable for the first year and reaching an MGI of 6.0 over the life of the building can be expected, which suggests a very heavy and dense mould coverage. However, the year when this heavy mould growth will occur cannot be estimated from the results of these simulations. Other key inferences of this study are:

- The maximum warm-up days input in EnergyPlus has an influence on MGI results;
- That the maximum mould growth is observed on the south facade, followed by the north, west, and east facades across the year. It is important to note that the predominant wind direction in this location is along the south side, followed by north, west, and east. It seems that this order of mould growth is based on the wind direction and the rain that is driven by the wind. It is also important to note that the HAMT does not account for the precipitation;
- Even during the driest month of the year, the average MGI does not fall below 2.5 due to the porous material property. Additionally, the porosity and density of the material plays an important role in mould growth. These material properties determine the dirt and dust that accumulates on the surface of the material, along with the moisture content of the building material, and provide enough nutrients for the mould to grow. However, this cannot be tested using a computer simulation;
- The surface temperature with the surface RH of the material plays a very important role in MGI, followed by outdoor DBT and RH, global horizontal radiation, as well as diffused horizontal radiation.

This study observes the lack of a database of hygrothermal properties of local building materials, not only in India, but across the world. Additionally, it is also important to note that the data and results presented here are only simulated, and the authors suggest that a field study should be conducted to further validate the results from this study. The results have only been validated by referring to the range of MGI that are available in the literature for similar climatic conditions and material properties. This study solely examines the mould-growth index and the parameters driving it, and only through computer-based simulations, which is one of the limitations of this study.

A novel finding of the study implies that hygrothermal properties should be considered, along with thermal properties, before recommending a building material as an energy conservation option. This because inadequate hygrothermal properties can contribute to mould growth and poor indoor air quality.

Author Contributions: Conceptualization, S.D.; methodology, S.D., A.K.S. and N.V.S.K.M.; software, N.V.S.K.M.; validation, S.D., A.K.S. and N.V.S.K.M.; formal analysis, S.D. and N.V.S.K.M.; investigation, S.D. and N.V.S.K.M.; resources, S.D., A.K.S., N.V.S.K.M. and G.P.; data curation, N.V.S.K.M.; writing—original draft preparation, S.D., A.K.S., N.V.S.K.M. and G.P.; writing—review and editing, S.D., N.V.S.K.M., A.K.S. and G.P.; visualization, N.V.S.K.M. and G.P.; supervision, A.K.S. and G.P.; funding acquisition, G.P. All authors have read and agreed to the published version of the manuscript.

Funding: This research received no external funding.

Data Availability Statement: The data that support the findings of this study are available from the corresponding authors upon reasonable request.

Acknowledgments: The authors are thankful to the Scopus database, Science Direct, Web of Science, and Google Scholar for Mould-Growth Study related publications. The authors are also thankful to the anonymous reviewers for their constructive suggestions to improve the quality of the present work.

Conflicts of Interest: The authors declare no conflict of interest.

References

1. Central Electricity Authority in India. Growth of Electricity Sector in India from 1947–2020. New Delhi. 2020. Available online: https://cea.nic.in/wp-content/uploads/pdm/2020/12/growth_2020.pdf (accessed on 2 January 2022).
2. Kumar, S.; Kamath, M.; Deshmukh, A.; Sarraf, S.; Seth, S.; Walia, A. Energy Conservation and Commercialization (ECO-III) Performance Based Rating and Energy Performance Benchmarking for Commercial Buildings in India. 2010. Available online: <https://www.buildingrating.org/file/1147/download?token=xcnAo2UNeBIV7cWW7xnZ2VhCvUPAJbZlJuejjV1okj0> (accessed on 6 January 2022).
3. Rawal, R.; Shukla, Y.; Didwania, S.; Singh, M.; Mewada, V. Residential Buildings in India: Energy Use Projections and Savings Potentials. 2014. Available online: https://www.gbpn.org/sites/default/files/03.INDIABaseline_ES_0.pdf (accessed on 9 January 2022).
4. Vrana, T. *Impact of Moisture on Long Term Performance of Insulating Products Based on Stone Wool*; KTH—The Royal Institute of Technology School of Architecture and the Built Environment: Stockholm, Sweden, 2007.
5. D’Agostino, D.; Landolfi, R.; Nicoletta, M.; Minichiello, F. Experimental Study on the Performance Decay of Thermal Insulation and Related Influence on Heating Energy Consumption in Buildings. *Sustainability* **2022**, *14*, 2947. [\[CrossRef\]](#)
6. Hao, L.; Herrera-Avellanosa, D.; Del Pero, C.; Troi, A. What Are the Implications of Climate Change for Retrofitted Historic Buildings? A Literature Review. *Sustainability* **2020**, *12*, 7557. [\[CrossRef\]](#)
7. World Health Organisation. *WHO Guidelines for Indoor Air Quality: Dampness and Mould*; World Health Organisation: Geneva, Switzerland, 2014; Available online: <https://www.who.int/publications/i/item/9789289041683> (accessed on 19 April 2022).
8. Kumar, S. *User Guide Energy Conservation Building Code*, 2nd ed.; Bureau of Energy Efficiency: Delhi, India, 2011.
9. Manivannan, S.; Venugopal, V.; Kindo, A.J.; Kuppaswamy, R. Method for assessment of indoor household dampness for its use in epidemiological studies in tropical settings. *Ann. Trop. Med. Public Health* **2017**, *10*, 1587–1590. [\[CrossRef\]](#)
10. Stephenson, L.D.; Heffron, A.; Mehnert, B.B.; Alvey, J.B.; Boddu, V.; Gao, E.J.; Lawrence, D.J.; Kumar, A. Prediction of Long Term Degradation of Insulating Materials. 2015. Available online: www.erc.usace.army.mil (accessed on 6 January 2022).
11. Hukka, A.; Viitanen, H.A. A mathematical model of mould growth on wooden material. *Wood Sci. Technol.* **1999**, *33*, 475–485. [\[CrossRef\]](#)
12. Madigan, M.T.; Martinko, J.M. *Brock Biology of Microorganisms*, 11th ed.; Pearson: London, UK, 2005; Volume 8, pp. 149–152.
13. *ASHRAE 160-2016*; Criteria for Design Analysis in Buildings. ASHRAE Standards Committee: Tullie Circle, NE, USA, 2016; Volume 8400.
14. Viitanen, H. *Factors Affecting Mould Growth on Kiln Dried Wood*; VTT: Espoo, UK, 2001; pp. 1–8.
15. Johansson, P.; Ekstrand-Tobin, A.; Svensson, T.; Bok, G. Laboratory study to determine the critical moisture level for mould growth on building materials. *Int. Biodeterior. Biodegradation* **2012**, *73*, 23–32. [\[CrossRef\]](#)
16. Macher, J.M.; Mendell, M.J.; Chen, W.; Kumagai, K. Development of a method to relate the moisture content of a building material to its water activity. *Indoor Air* **2017**, *27*, 599–608. [\[CrossRef\]](#)
17. Adan, O.C.; Samson, R.A. *Fundamentals of Mold Growth in Indoor Environments and Strategies for Healthy Living*; Wageningen Academic Publishers: Wageningen, The Netherlands, 2011.
18. Morse, R. Indoor Air Quality and Mold Prevention of the Building Envelope | WBDG—Whole Building Design Guide. 2017. Available online: <https://www.wbdg.org/resources/indoor-air-quality-and-mold-prevention-building-envelope> (accessed on 1 May 2021).
19. Baughman, A.V.; Arens, E.A. Indoor Humidity and Human Health—Part I: Literature Review of Health Effects of Humidity-Influenced Indoor Pollutants. *ASHRAE Trans.* **1996**, *102*, 193–211. Available online: https://www.researchgate.net/publication/292036403_Indoor_humidity_and_human_health_-_Part_I_Literature_review_of_health_effects_of_humidity-influenced_indoor_pollutants (accessed on 10 January 2022).
20. Ayerst, G. The effects of moisture and temperature on growth and spore germination in some fungi. *J. Stored Prod. Res.* **1969**, *5*, 127–141. [\[CrossRef\]](#)
21. Adan, O.C.G. *On the Fungal Defacement of Interior Finishes*; Technische Universiteit Eindhoven: Eindhoven, The Netherlands, 1994; pp. 127–141. [\[CrossRef\]](#)
22. Sedlbauer, K. *Prediction of Mould Fungus Formation on the Surface of/and Inside Building Components*; Fraunhofer Institute for Building Physics: Stuttgart, Germany, 2001.
23. Zhang, X.; Liang, J.; Wang, B.; Lv, Y.; Xie, J. Indoor Air Design Parameters of Air Conditioners for Mold-Prevention and Antibacterial in Island Residential Buildings. *Int. J. Environ. Res. Public Health* **2020**, *17*, 7316. [\[CrossRef\]](#)
24. Viitanen, H.A. Modelling the Time Factor in the Development of Brown Rot Decay in Pine and Spruce Sapwood—The Effect of Critical Humidity and Temperature Conditions. *Holzforschung* **1997**, *51*, 99–106. [\[CrossRef\]](#)

25. Viitanen, H.; Hanhijärvi, A.; Hukka, A.; Koskela, K. Modelling mould growth and decay damages. In Proceedings of the in Healthy Buildings 2000, Espoo, Finland, 6–10 August 2000; pp. 341–346.
26. Viitanen, H.; Ritschkoff, A.C. Mould growth in pine and spruce sapwood in relation to air humidity and temperature. *Environ. Sci.* **1991**, *49*.
27. Clarke, J.; Johnstone, C.; Kelly, N.; McLean, R.; Anderson, J.; Rowan, N.; Smith, J. A technique for the prediction of the conditions leading to mould growth in buildings. *Build. Environ.* **1999**, *34*, 515–521. [[CrossRef](#)]
28. Moon, H.J. *Assessing Mold Risks in Buildings under Uncertainty*; Georgia Institute of Technology: Atlanta, GA, USA, 2005.
29. Vinha, J.; Salminen, K.; Viitanen, H.; Ojanen, T. Mathematical analysis of mould growth risk in building envelopes. In Proceedings of the CIB W40 Building Science Forum 2006, Syracuse, NY, USA, 5–6 September 2006.
30. Simon, P.; Philip, B.; Som, S.; Joshua, N.; Mark, A. State-of-the-Art for Hygrothermal Simulation Tools. 2017. Available online: <https://info.ornl.gov/sites/publications/Files/Pub73069.pdf> (accessed on 20 January 2022).
31. Ritschkoff, A.-C.; Viitanen, H.; Koskela, K. The response of building materials to the mould exposure at different humidity and temperature conditions. In Proceedings of the in Healthy Buildings 2000, Espoo, Finland, 6–10 August 2000; pp. 317–322.
32. Nielsen, K.F.; Holm, G.; Uttrup, L.; Nielsen, P. Mould growth on building materials under low water activities. Influence of humidity and temperature on fungal growth and secondary metabolism. *Int. Biodeterior. Biodegrad.* **2004**, *54*, 325–336. [[CrossRef](#)]
33. Viitanen, H.; Vinha, J.; Salminen, K.; Ojanen, T.; Peuhkuri, R.; Paaajanen, L.; Lähdesmäki, K. Moisture and Bio-deterioration Risk of Building Materials and Structures. *J. Build. Phys.* **2010**, *33*, 201–224. [[CrossRef](#)]
34. Grant, C.; Hunter, C.; Flannigan, B.; Bravery, A. The moisture requirements of moulds isolated from domestic dwellings. *Int. Biodeterior. Biodegrad.* **1989**, *25*, 259–284. [[CrossRef](#)]
35. Andersen, B.; Frisvad, J.C.; Søndergaard, I.; Rasmussen, I.S.; Larsen, L.S. Associations between Fungal Species and Water-Damaged Building Materials. *Appl. Environ. Microbiol.* **2011**, *77*, 4180–4188. [[CrossRef](#)] [[PubMed](#)]
36. Flannigan, B.; Samson, R.; Miller, J. *Microorganisms in Home and Indoor Work Environments: Diversity, Health Impacts, Investigation and Control*, 2nd ed.; CRC Press LLC: New York, NY, USA, 2011.
37. Viitanen, H.; Ojanen, T. Improved model to predict mold growth in building materials. In Proceedings of the Thermal Performance of Exterior Envelopes of Whole Buildings X International Conference, Clearwater Beach, FL, USA, 2 December 2007.
38. Abuku, M.; Janssen, H.; Roels, S. Impact of wind-driven rain on historic brick wall buildings in a moderately cold and humid climate: Numerical analyses of mould growth risk, indoor climate and energy consumption. *Energy Build.* **2009**, *41*, 101–110. [[CrossRef](#)]
39. Chen, W.; Claridge, D.E.; Rohrs, C.; Liao, J. Modeling to predict positive pressurization required to control mold growth from infiltration in buildings in a hot and humid climate. *Build. Environ.* **2016**, *104*, 102–113. [[CrossRef](#)]
40. Møller, E.B.; Andersen, B.; Rode, C.; Peuhkuri, R. Conditions for mould growth on typical interior surfaces. *Energy Procedia* **2017**, *132*, 171–176. [[CrossRef](#)]
41. Jain, A. Molds in building materials of Agra (India) at various humidity conditions. *Relat. Humidity Sens. Manag. Environ. Eff.* **2011**, 137–156.
42. Kočí, V.; Vejmelková, E.; Čáchová, M.; Koňáková, D.; Keppert, M.; Maděra, J.; Černý, R. Effect of Moisture Content on Thermal Properties of Porous Building Materials. *Int. J. Thermophys.* **2016**, *38*, 28. [[CrossRef](#)]
43. Choi, H.-J.; Kang, J.-S.; Huh, J.-H. A Study on Variation of Thermal Characteristics of Insulation Materials for Buildings According to Actual Long-Term Annual Aging Variation. *Int. J. Thermophys.* **2018**, *39*, 1–11. [[CrossRef](#)]
44. Kamperidou, V. The Biological Durability of Thermally- and Chemically-Modified Black Pine and Poplar Wood Against Basidiomycetes and Mold Action. *Forests* **2019**, *10*, 1111. [[CrossRef](#)]
45. Rawal, R. Thermal Performance of Walling Material and Wall Technology. June. 2020. Available online: https://www.gkspl.in/wp-content/uploads/2020/07/Thermal-performance-of-walling-material-and-wall-Technology_Part-12_V2.pdf (accessed on 28 February 2022).
46. Zarr, R.R.; Dalton, G.R.; Fioravante, S.M. Development of a NIST Standard Reference Database for Thermal Conductivity of Building Materials. 2000. Available online: <https://www.nist.gov/publications/development-nist-standard-reference-database-thermal-conductivity-building-materials> (accessed on 18 January 2022).
47. International Finance Corporation. *India Construction Materials Database of Embodied Energy and Global Environmental Indicators for Materials Warming Potential Methodology & Results Version 1.0*; Methodology Report; International Finance Corporation: Washington, DC, USA, 2017; pp. 1–100.
48. Bhatnagar, M.; Mathur, J.; Garg, V. Development of reference building models for India. *J. Build. Eng.* **2019**, *21*, 267–277. [[CrossRef](#)]
49. Bureau of Energy Efficiency. Energy Conservation Building Code. 2017. Available online: https://beeindia.gov.in/sites/default/files/BEE_ECBC2017.pdf (accessed on 22 January 2022).
50. Antretter, F.; Simon, P. HAMT Extension for EnergyPlus Encompasses Moisture Sources Due to Air Leakage. 2019. Available online: <https://www.osti.gov/biblio/1494004#:~:text=Extending%20the%20EnergyPlus%20HAMT%20model,to%20be%20assessed%20with%20EnergyPlus.&text=Overall%2C%20the%20new%20model%20is,of%20the%20existing%20HAMT%20model> (accessed on 25 January 2022).
51. ISO 12571:2013; Hygrothermal performance of building materials and products—Determination of hygroscopic Sorption Properties (ISO 12571:2013). BSI Standards Limited. ISO: Geneva, Switzerland, 2013.

52. Kumaran, M.K. *Heat, Air and Moisture Transfer in Insulated Envelope Parts: Task 3—Material Properties*; Laboratorium Bouwfysica, Departement Burgerlijke Bouwkunde, K.U.: Leuven, Belgium, 1996.
53. Berkeley Lab. Warmup Convergence: Engineering Reference—EnergyPlus 8.0. 2014. Available online: <https://bigladdersoftware.com/epx/docs/8-0/engineering-reference/page-006.html> (accessed on 13 June 2022).
54. Judkoff, R.; Neymark, J. Model validation and testing: The methodological foundation of ASHRAE Standard 140. *ASHRAE Trans.* **2006**, *112 Pt 2*, 367–376.
55. Menneer, T.; Mueller, M.; Sharpe, R.A.; Townley, S. Modelling mould growth in domestic environments using relative humidity and temperature. *Build. Environ.* **2021**, *208*, 108583. [[CrossRef](#)]
56. Ahmad, M.R.; Chen, B.; Maierdan, Y.; Kazmi, S.M.S.; Munir, M.J. Study of a new capillary active bio-insulation material by hygrothermal simulation of multilayer wall. *Energy Build.* **2021**, *234*, 110724. [[CrossRef](#)]
57. Kang, Y.; Kim, S. Evaluation of Indoor Hygrothermal Performance with the Heat and Moisture Transport in Walls. *SSRN* **2022**, 4047762, 24. [[CrossRef](#)]